JOURNAL OF AIRCRAFT
Vol. 41, No. 1, January–February 2004

Design of the Blended Wing Body Subsonic Transport

R. H. Liebeck*
The Boeing Company, Huntington Beach, California 92647

The Boeing Blended-Wing–Body (BWB) airplane concept represents a potential breakthrough in subsonic transport efficiency. Work began on this concept via a study to demonstrate feasibility and begin development of this new class of airplane. In this initial study, 800-passenger BWB and conventional configuration airplanes were sized and compared for a 7000-n mile design range. Both airplanes were based on engine and structural (composite) technology for a 2010 entry into service. Results showed remarkable performance improvements of the BWB over the conventional baseline, including a 15% reduction in takeoff weight and a 27% reduction in fuel burn per seat mile. Subsequent in-house studies at Boeing have yielded the development of a family of BWB transports ranging from 200 to 600 passengers with a high level of parts commonality and manufacturing efficiency. Studies have also demonstrated that the BWB is readily adaptable to cruise Mach numbers as high as 0.95. The performance improvement of the latest Boeing BWBs over conventional subsonic transports based on equivalent technology has increased beyond the predictions of the early NASA-sponsored studies.

I. Introduction

IT is appropriate to begin with a reference to the Wright Flyer itself, designed and first flown in 1903. A short 44 years later, the swept-wing Boeing B-47 took flight. A comparison of these two airplanes shows a remarkable engineering accomplishment within a period of slightly more than four decades. Embodied in the B-47 are most of the fundamental design features of a modern subsonic jet transport: swept wing and empennage and podded engines hung on pylons beneath and forward of the wing. The Airbus A330, designed 44 years after the B-47, appears to be essentially equivalent, as shown in Fig. 1.

Thus, in 1988, when NASA Langley Research Center's Dennis Bushnell asked the question: "Is there a renaissance for the long-haul transport?" there was cause for reflection. In response, a brief preliminary design study was conducted at McDonnell Douglas to create and evaluate alternate configurations. A preliminary configuration concept, shown in Fig. 2, was the result. Here, the pressurized passenger compartment consisted of adjacent parallel tubes, a lateral extension of the double-bubble concept. Comparison with a conventional configuration airplane sized for the same design mission indicated that the blended configuration was significantly lighter, had a higher lift to drag ratio, and had a substantially lower fuel burn.

This paper is intended to chronicle the technical development of the Blended-Wing–Body (BWB) concept. Development is broken into three somewhat distinct phases: formulation, initial development and feasibility, and, finally, a description of the current Boeing BWB baseline airplane.

II. Formulation of the BWB Concept

The performance potential implied by the blended configuration provided the incentive for NASA Langley Research Center to fund a small study at McDonnell Douglas to develop and compare advanced technology subsonic transports for the design mission of 800 passengers and a 7000-n mile range at a Mach number of 0.85. Composite structure and advanced technology turbofans were utilized.

Defining the pressurized passenger cabin for a very large airplane offers two challenges. First, the square-cube law shows that the cabin surface area per passenger available for emergency egress decreases with increasing passenger count. Second, cabin pressure loads are most efficiently taken in hoop tension. Thus, the early study began with an attempt to use circular cylinders for the fuselage pressure vessel, as shown in Fig. 3, along with the corresponding first cut at the airplane geometry. The engines are buried in the wing root, and it was intended that passengers could egress from the sides of both the upper and lower levels. Clearly, the concept was headed back to a conventional tube and wing configuration. Therefore, it was decided to abandon the requirement for taking pressure loads in hoop tension and to assume that an alternate efficient structural concept could be developed. Removal of this constraint became pivotal for the development of the BWB.

Passenger cabin definition became the origin of the design, with the hoop tension structural requirement deleted. Three canonical forms shown in Fig. 4a, each sized to hold 800 passengers, were considered. The sphere has minimum surface area; however, it is not streamlined. Two canonical streamlined options include the conventional cylinder and a disk, both of which have nearly equivalent surface area. Next, each of these fuselages is placed on a wing that has a total surface area of 15,000 ft^2. Now the effective masking of the wing by the disk fuselage results in a reduction of total aerodynamic wetted area of 7000 ft^2 compared to the cylindrical fuselage plus wing geometry, as shown in Fig. 4b. Next, adding engines (Fig. 4c) provides a difference in total wetted area of 10,200 ft^2. (Weight and balance require that the engines be located aft on the disk configuration.) Finally, adding the required control surfaces to each configuration as shown in Fig. 4d results in a total wetted area difference of 14,300 ft^2, or a reduction of 33%. Because the cruise lift to drag ratio is related to the wetted area aspect ratio, b^2/S_{wet}, the BWB configuration implied a substantial improvement in aerodynamic efficiency.

The disk fuselage configuration sketched in Fig. 4d has been used to describe the germination of the BWB concept. Synergy of the basic disciplines is strong. The fuselage is also a wing, an inlet for the engines, and a pitch control surface. Verticals provide directional stability, control, and act as winglets to increase the effective aspect ratio. Blending and smoothing the disk fuselage into the wing achieved transformation of the sketch into a realistic airplane configuration. In addition, a nose bullet was added to offer cockpit visibility. This also provides additional effective wing chord at the centerline to offset compressibility drag due to the unsweeping of the isobars at the plane of symmetry.

Modern supercritical airfoils with aft camber and divergent trailing edges were assumed for the outer wing, whereas the centerbody was to be based on a reflexed airfoil for pitch trim. A proper spanload implies a relatively low lift coefficient due to the very large centerbody chords. Therefore, airfoil LW102A was designed for $c_l = 0.25$

Received 9 June 2002; revision received 19 December 2002; accepted for publication 10 January 2003.

*Boeing Senior Technical Fellow, Phantom Works. Fellow AIAA.

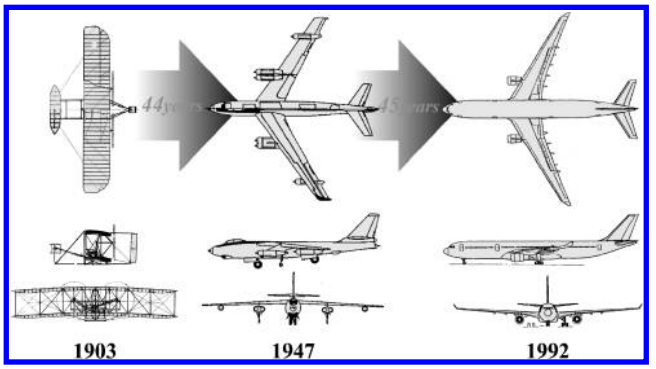

Fig. 1 Aircraft design evolution, the first and second 44 years.

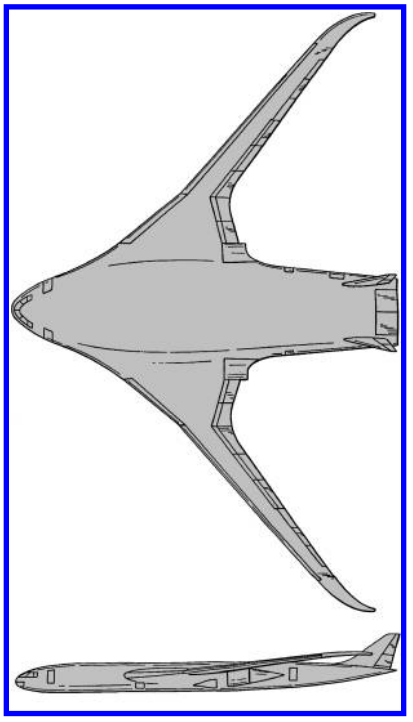

Fig. 2 Early blended configuration concept.

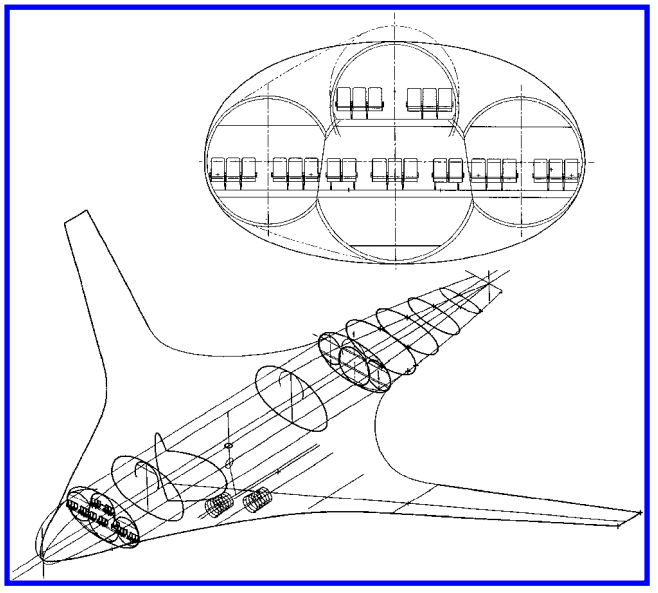

Fig. 3 Early configuration with cylindrical pressure vessel and engines buried in the wing root.

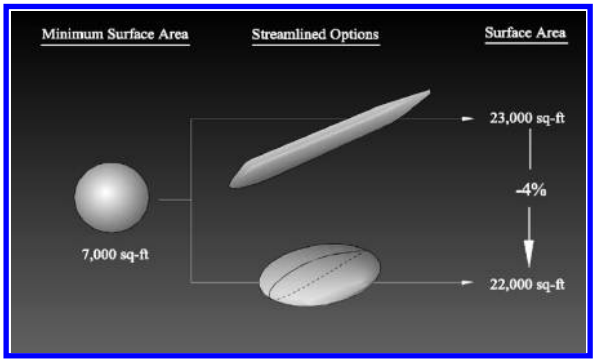

a) Effect of body type on surface area

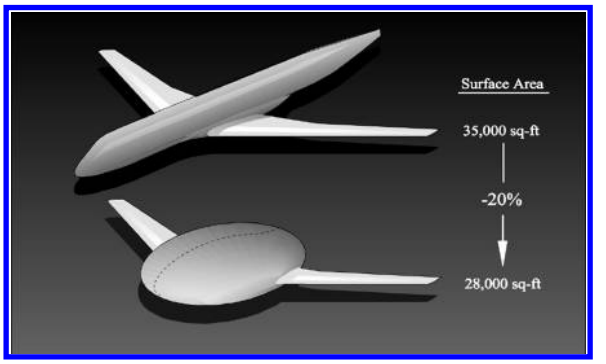

b) Effect of wing/body integration on surface area

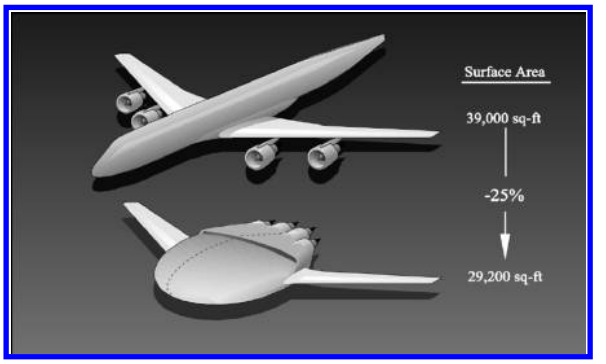

c) Effect of engine installation on surface area

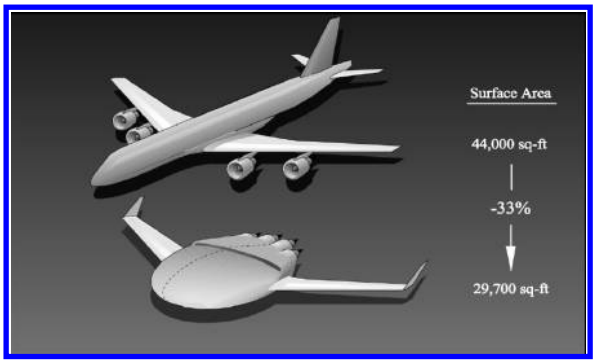

d) Effect of controls integration on surface area

Fig. 4 Genesis of the BWB concept.

and $c_{mc/4} = +0.03$ at $M = 0.7$ using the method of Ref. 1. The resulting airfoil section is shown in Fig. 5, along with a planform indicating how pitch trim is accomplished via centerbody reflex, whereas the outboard wing carries a proper spanload all of the way to the wingtip. Blending of this centerbody airfoil with the outboard supercritical sections yielded an aerodynamic configuration with a nearly elliptic spanload. At this early stage of BWB development, the structurally rigid centerbody was regarded as offering free wingspan. Outer wing geometry was essentially taken from a

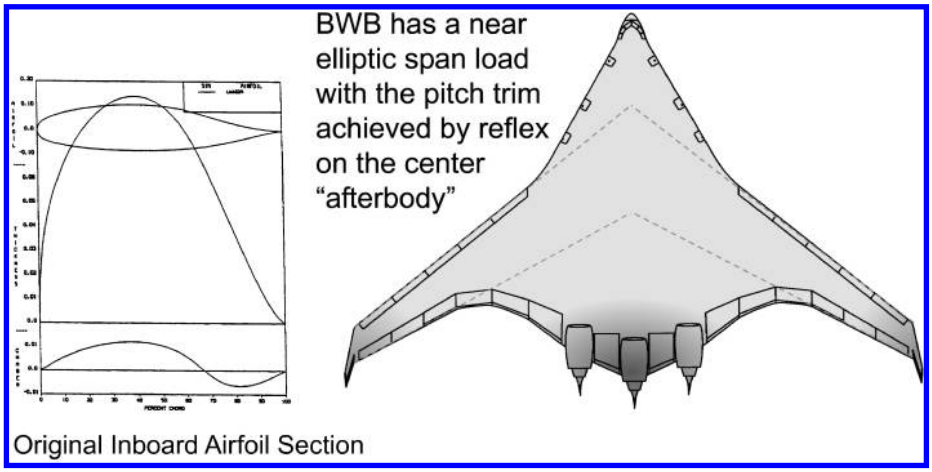

Fig. 5 Original centerbody airfoil LW109A and planform showing pitch trim effector.

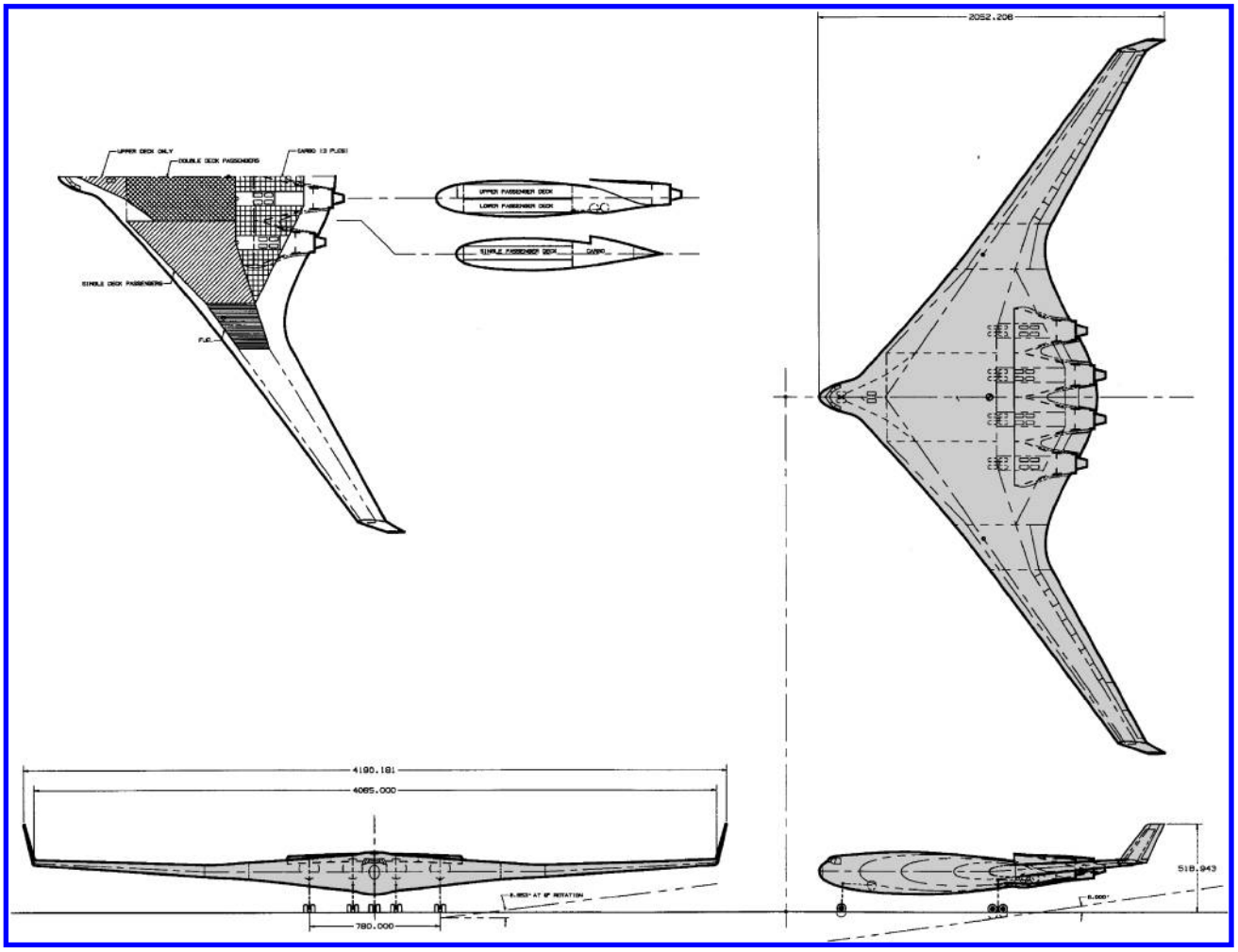

Fig. 6 First-generation BWB.

conventional transport and bolted to the side of the centerbody. The result was a wingspan of 349 ft, a trapezoidal aspect ratio of 12, and a longitudinal static margin of −15%, implying a requirement for a fly-by-wire control system.

The aft engine location, dictated by balance requirements, offered the opportunity for swallowing the boundary layer from that portion of the centerbody upstream of the inlet, a somewhat unique advantage of the BWB configuration. In principle, boundary-layer swallowing can provide improved propulsive efficiency by reducing the ram drag, and this was the motivation for the wide “mail-slot” inlet sketched in Fig. 6. However, this assumed that such an inlet could be designed to provide uniform flow and efficient pressure recovery at the fan face of the engine(s).

Two structural concepts (Fig. 7) were considered for the centerbody pressure vessel. Both required that the cabin be composed of longitudinal compartments to provide for wing ribs 150 in. apart to

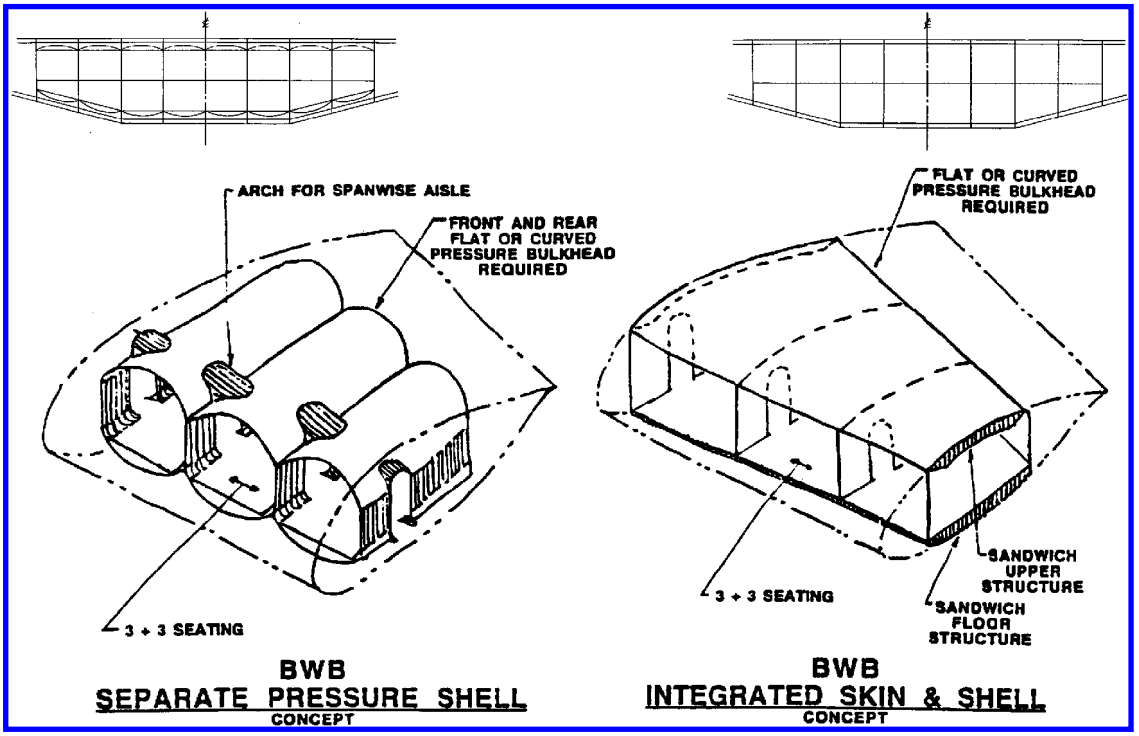

Fig. 7 Centerbody pressure vessel structural concepts.

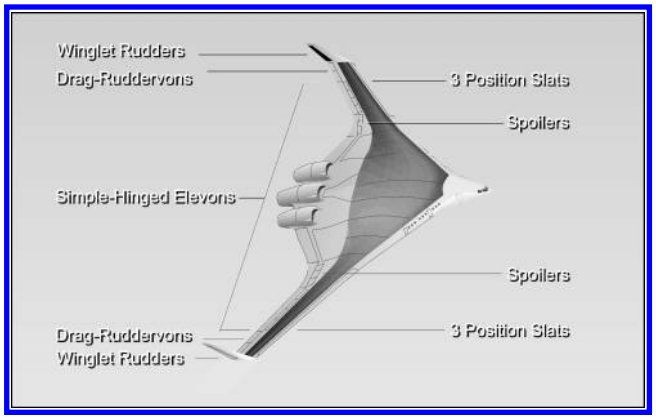

Fig. 8 Flight control system architecture of the first-generation BWB.

carry the pressure load. The first concept used a thin, arched pressure vessel above and below each cabin, where the pressure vessel skin takes the load in tension and is independent of the wing skin. A thick sandwich structure for both the upper and lower wing surfaces was the basis for the second concept. In this case, both cabin pressure loads and wing bending loads are taken by the sandwich structure. A potential safety issue exists with the separate arched pressure vessel concept. If a rupture were to occur in the thin arched skin, the cabin pressure would have to be borne by the wing skin, which must in turn be sized to carry the pressure load. Thus, once the wing skin is sized by this condition, in principle there is no need for the inner pressure vessel. Consequently, the thick sandwich concept was chosen for the centerbody structure. A three-view of the original BWB is given in Fig. 6, and a description of the packaging of the interior is also shown there. Passengers are carried in both single and double deck cabins, and the cargo is carried aft of the passenger cabin. As a tailless configuration, the BWB is a challenge for flight mechanics, and the early control system architecture is shown in the isometric view in Fig. 8. A complete description of original BWB study is given in Ref. 2. Future generations of BWB designs would begin to address constraints not observed by this initial concept, but the basic character of the aircraft persists to this day.

III. BWB Design Constraints

As an integrated airplane configuration, the BWB must satisfy a unique set of design requirements. Included are the following:

A. Volume

Passengers, cargo, and systems must be packaged within the wing itself. This leads to a requirement for the maximum thickness-to-chord ratio on the order of 17%, a value that is much higher than is typically associated with transonic airfoils.

B. Cruise Deck Angle

Because the passenger cabin is packaged within the centerbody, the centerbody airfoils must be designed to generate the necessary lift at an angle of attack consistent with cabin deck angle requirements (typically less than 3 deg). Taken by itself, this requirement suggests the use of positive aft camber on the centerbody airfoils.

C. Trim

A BWB configuration is considered trimmed (at the nominal cruise condition) when the aerodynamic center of pressure is coincident with the center of gravity, and all of the trailing-edge control surfaces are faired. Positive static stability requires that the nose-down pitching moment be minimized. This limits the use of positive aft camber and conflicts with the preceding deck angle requirement.

D. Landing Approach Speed and Attitude

BWB trailing-edge control surfaces cannot be used as flaps because the airplane has no tail to trim the resulting pitching moments. Trailing-edge surface deflection is set by trim requirements, rather than maximum lift. Therefore, the maximum lift coefficient of a BWB will be lower than that of a conventional configuration, and, hence, the wing loading of a BWB will be lower. Also, because there are no flaps, the BWB's maximum lift coefficient will occur at a relatively large angle of attack, and the flight attitude during approach is correspondingly high.

E. Buffet and Stall

The BWB planform causes the outboard wing to be highly loaded. This puts pressure on the wing designer to increase both the outboard

wing chord and washout, which degrades cruise performance. A leading-edge slat is required outboard for low-speed stall protection. These issues apply to a conventional configuration, but they are exacerbated by the BWB planform.

F. Power for Control Surface Actuation

Tailless configurations have short moment arms for pitch and directional control, and, therefore, multiple, large, rapidly moving control surfaces are required. Trailing-edge devices and winglet rudders are called on to perform a host of duties, including basic trim, control, pitch stability augmentation, and wing load alleviation. Because some of the control surfaces can perform multiple functions (e.g., outboard elevon/drag rudder offers pitch, roll, and yaw authority), control surface allocation becomes a critical issue. The mere size of the inboard control surfaces implies a constraint on the airfoil design to minimize hinge moments. Hinge moments are related to the scale of the control surface as follows: The area increases as the square of the scale, and, in turn, the moment increases with the cube of the scale. Once the hydraulic system is sized to meet the maximum hinge moment, the power requirement becomes a function of rate at which a control surface is moved.

If the BWB is designed with a negative static margin (unstable), it will require active flight control with a high bandwidth, and the control system power required may be prohibitive. Alternatively, designing the airplane to be stable at cruise requires front-loaded airfoils, washout, and limited (if any) aft camber. This implies a higher angle of attack, which, in turn, threatens the deck angle constraint.

G. Manufacturing

The aerodynamic solution to the design constraints just listed can readily result in a complex three-dimensional shape that would be difficult and expensive to produce. Therefore, the aerodynamicist must strive for smooth, simply curved surfaces that at the same time satisfy the challenging set of constraints just described.

IV. Initial Development and Feasibility

A NASA/industry/university team was formed in 1994 to conduct a three-year study to demonstrate the technical and commercial feasibility of the BWB concept. McDonnell Douglas was the Program Manager, and the team members included NASA Langley Research Center, NASA John H. Glenn Research Center at Lewis Field, Stanford University, the University of Southern California, the University of Florida, and Clark-Atlanta University. The original 800-passenger 7000-n mile design mission was retained. This work is summarized in Ref. 3.

A. Configuration Definition and Sizing

This study began with a refined sizing of the initial BWB configuration (Fig. 6), where minimum takeoff gross weight (TOGW) was set as the figure of merit. Primary constraints included an 11,000-ft takeoff field length, 150-kn approach speed, low-speed trimmed $C_{L\,\max}$ of 1.7, and a cruise Mach number of 0.85. Initial cruise altitude (ICA) was allowed to vary to obtain minimum TOGW, but with the requirement that the ICA be at least 35,000 ft. This yielded a trapezoidal wing of aspect ratio of 10, with a corresponding span of 280 ft and an area of 7840 ft^2. The resulting trapezoidal wing loading was on the order of 100 lb/ft^2, substantially lower than the 150 lb/ft^2 typical of modern subsonic transports. An explanation offered was that a significant portion of the trapezoidal wing is in effect hidden by the centerbody, and, therefore, the cost of trapezoidal wing area on airplane drag is reduced. This in turn allowed the airplane to optimize with a larger trapezoidal area to increase span with a relatively low cost on weight. A three-view and isometric of the resulting second-generation BWB is given in Fig. 9.

The double-deck BWB interior was configured with 10 150-in. wide passenger cabin bays, as shown in Fig. 10, with cargo compartments located outboard of the passenger bays and fuel in the wing, outboard of the cargo. Considerations and constraints included weight and balance, maximum offset of the passengers from the vehicle centerline (ride quality) and the external area of the cabin. Because this is the surface area of the pressure vessel, the extent of this area has a significant effect on the structural weight of the centerbody. The cabin partitions are in fact, wing ribs that are part of the primary structure. Windows were located in the leading edge on both decks, and the galleys and lavatories were located aft to help provide the passengers with an unobstructed forward view. Egress was via the main cabin doors in the leading edge, and through aft doors in the rear spar.

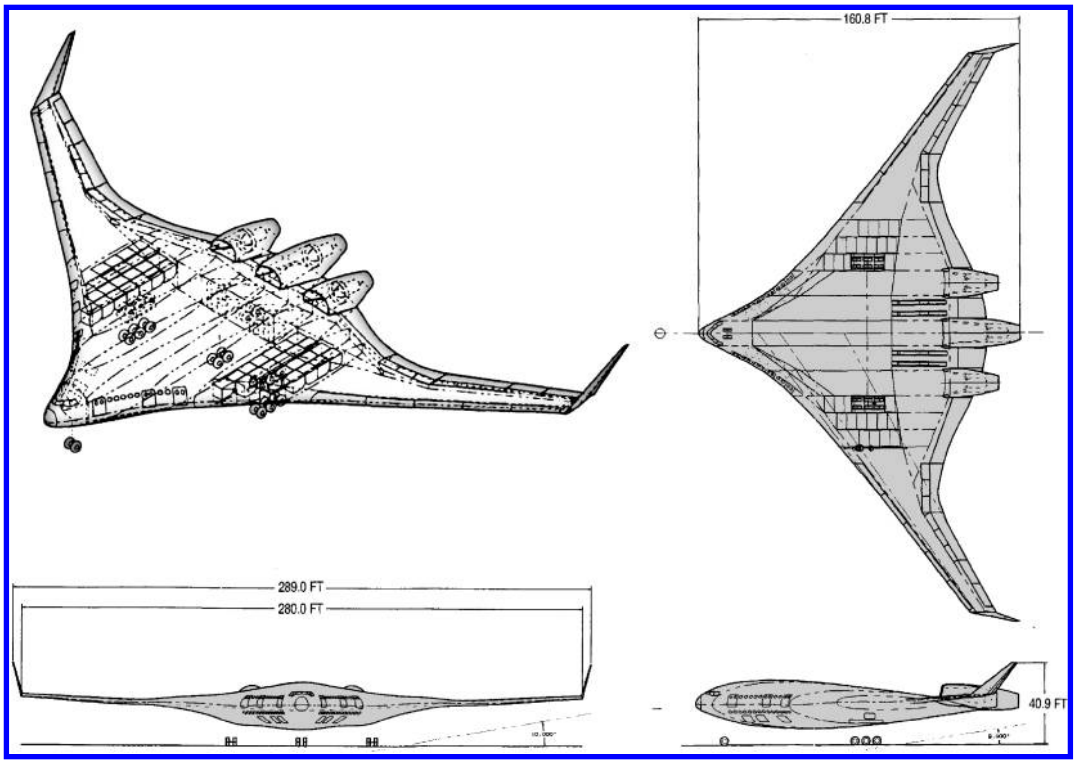

Fig. 9 Second-generation BWB.

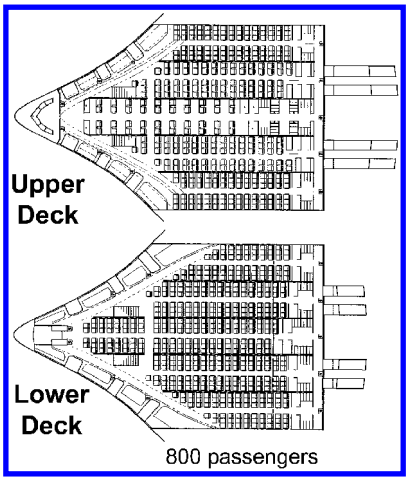

Fig. 10 Interior arrangement of passenger cabin.

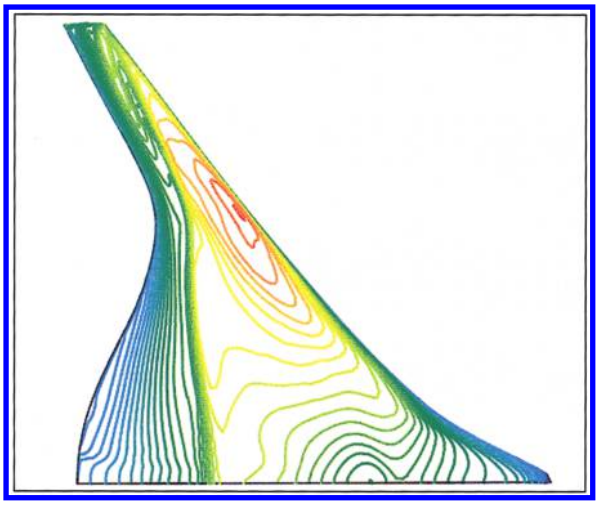

Fig. 12 Navier–Stokes computed upper surface pressure distributions.

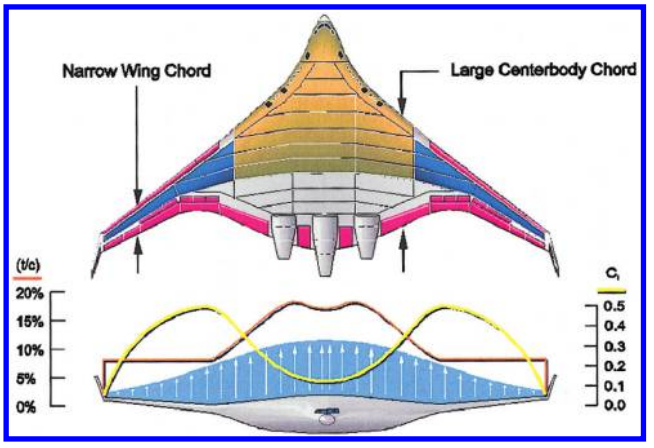

Fig. 11 Section lift coefficient and thickness-to-chord ratio variation with span.

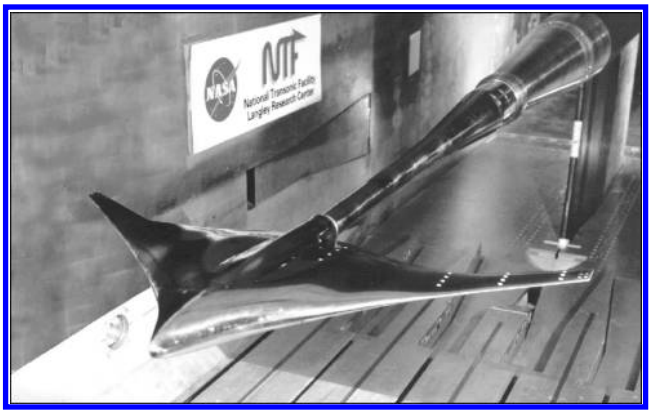

Fig. 13 BWB in the NASA LaRC NTF.

B. Aerodynamics

Some insight into the aerodynamic design of the BWB is provided in Fig. 11, where the trade between wing chord, thickness, and lift coefficient is shown. The outboard wing is moderately loaded, similar to a conventional configuration, where drag is minimized with a balance between the wetted area and shock strength. Moving inboard, the centerbody, with its very large chord, calls for correspondingly lower section lift coefficients to maintain an elliptic spanload. The low section lift requirement allows the very thick airfoils for packaging the passenger compartment and trailing-edge reflex for pitch trim.

Navier–Stokes computational fluid dynamics (CFD) methodology in both the inverse design and direct solution modes was employed to define the final BWB geometry. A solution showing the pressure distribution at the midcruise condition is shown in Fig. 12. The typical shock on the outboard wing is smeared into a compression wave on the centerbody. The flow pattern on the centerbody remained essentially invariant with angle of attack, and flow separation is initiated in the kink region between the outboard wing and the centerbody. Outer wing flow remains attached, providing lateral control into the stall regime. Similarly, the flow over the centerbody remains attached and provides a nearly constant flow environment for the engine inlets. This flow behavior is a consequence of significant lateral flow on the centerbody that provides a three-dimensional relief of compressibility effects. However, the relief on the centerbody is traded for a transonically stressed flow environment in the kink region. This is the ideal spanwise location for the stall to begin, from a flight mechanics point of view: The ailerons remain effective, and pitch-up is avoided.

C. Wind-Tunnel Tests

Transonic and low-speed wind-tunnel tests of the BWB configuration (Fig. 9) were conducted at NASA Langley Research Center (LaRC) in the National Transonic Facility (NTF), and this represented an invaluable opportunity to test at close to the full-scale Reynolds number. Figure 13 shows the BWB model mounted in the tunnel, and NTF results are compared with CFD predictions in Fig. 14. Excellent agreement for lift, drag, and pitching moment, as well as wing pressure distributions, is shown, including up to and beyond buffet onset. A primary objective of the test was to establish the effectiveness of the current state-of-the-art CFD methods for predicting the aerodynamic characteristics of a BWB airplane. The remarkable agreement indicated that CFD could be reliably utilized for the aerodynamic design and analysis.

A low-speed test of a powered 4% scale BWB was conducted in the NASA LaRC 14 × 22 foot wind tunnel (Fig. 15). Results verified trimmed $C_{L\,\max}$ estimates, showed favorable stall characteristics, and showed excellent control power through stall. Power effects were found to be much smaller than expected.

D. Stability and Control

During development of the second-generation BWB, it was assumed and accepted that the airplane would be statically unstable to achieve high cruise efficiency (L/D). Balance of the airplane was achieved by sliding the wing fore and aft on the centerbody, much like the procedure for a conventional configuration. However, this was clearly a more complex process due to the integrated nature of the BWB. The low effective wing loading meant that trailing-edge flaps would not be required, but a leading-edge slat on the outboard wing is required for the same reason as that on a conventional

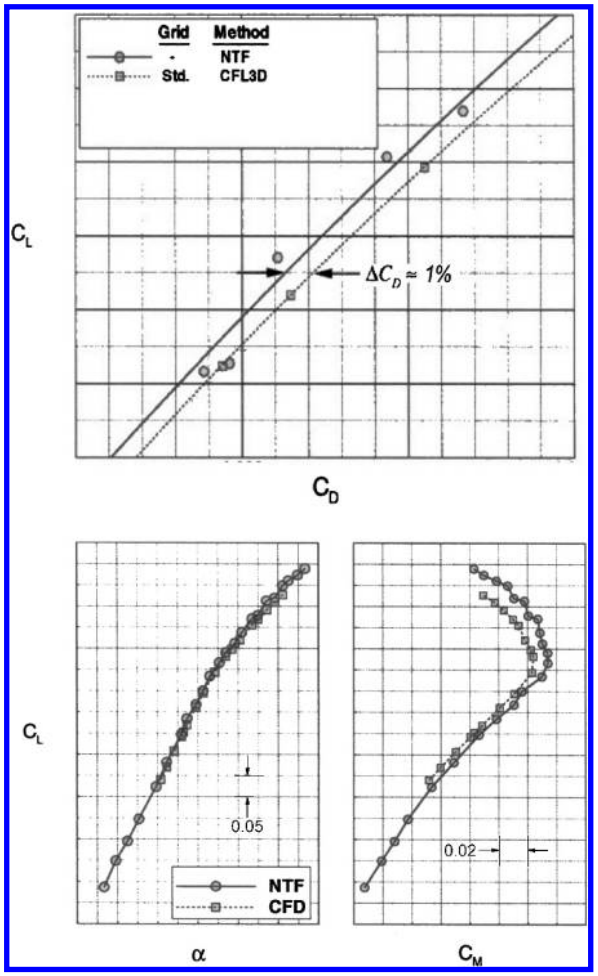

Fig. 14 Comparison of CFD predictions with NTF wind tunnel results.

Fig. 15 Powered BWB model in the NASA LaRC 14 × 22 foot tunnel for low-speed test.

airplane. The simple-hinged trailing-edge control surfaces function as elevons. Flight-critical stability augmentation and envelope protection was considered a requirement.

The outboard elevons are the primary pitch and roll controls because they have the largest lever arm about the center of gravity. Figure 16 shows the pitch authority of the individual elevons, as well as the locus of their effective centers of pressure. Note that they yield relatively short lever arms about the center of gravity, and even shorter lever arms about the landing gear for takeoff rotation. However, total control power is substantial due to the full span of elevons. The winglets with rudders provide primary directional stability and control. For the low-speed engine-out condition, the outboard elevons become split drag rudders, similar to those on the B-2, as shown in Fig. 17.

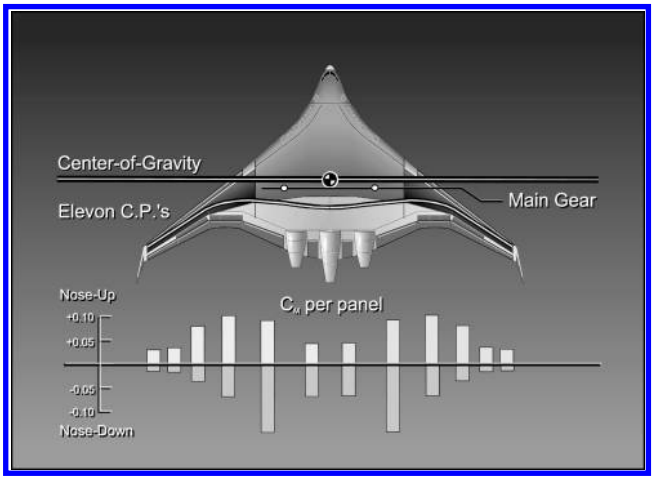

Fig. 16 Elevon effectiveness in pitch.

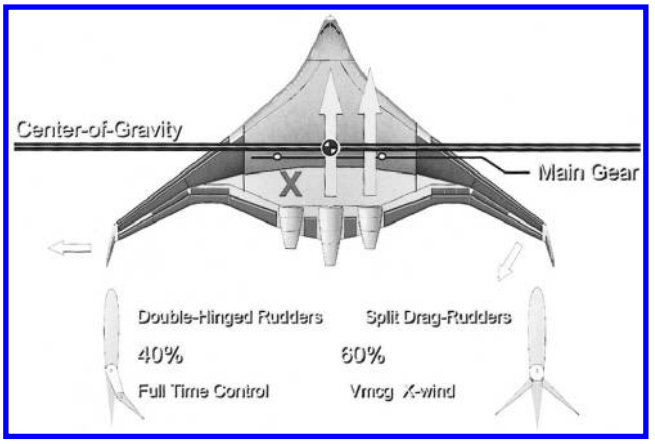

Fig. 17 Yaw control.

Fig. 18 Flight control testbed built by Stanford University.

E. Flight Demonstrator

Low-speed flight mechanics were explored with a 6% scale flight control testbed (Fig. 18), built at Stanford University under NASA sponsorship. Called the BWB-17, the airplane had a 17-ft wingspan, weighed 120 lb and was powered by two 35-cm^3 two-stroke engines with propellers. The model was dynamically scaled to match the flight characteristics of the full-scale BWB. Stability augmentation was provided by an onboard computer, which also recorded flight-test parameters. The first flight of the BWB-17 took place on 29 July 1997, at El Mirage Dry Lake in California. Excellent handling qualities were demonstrated within the normal flight envelope.

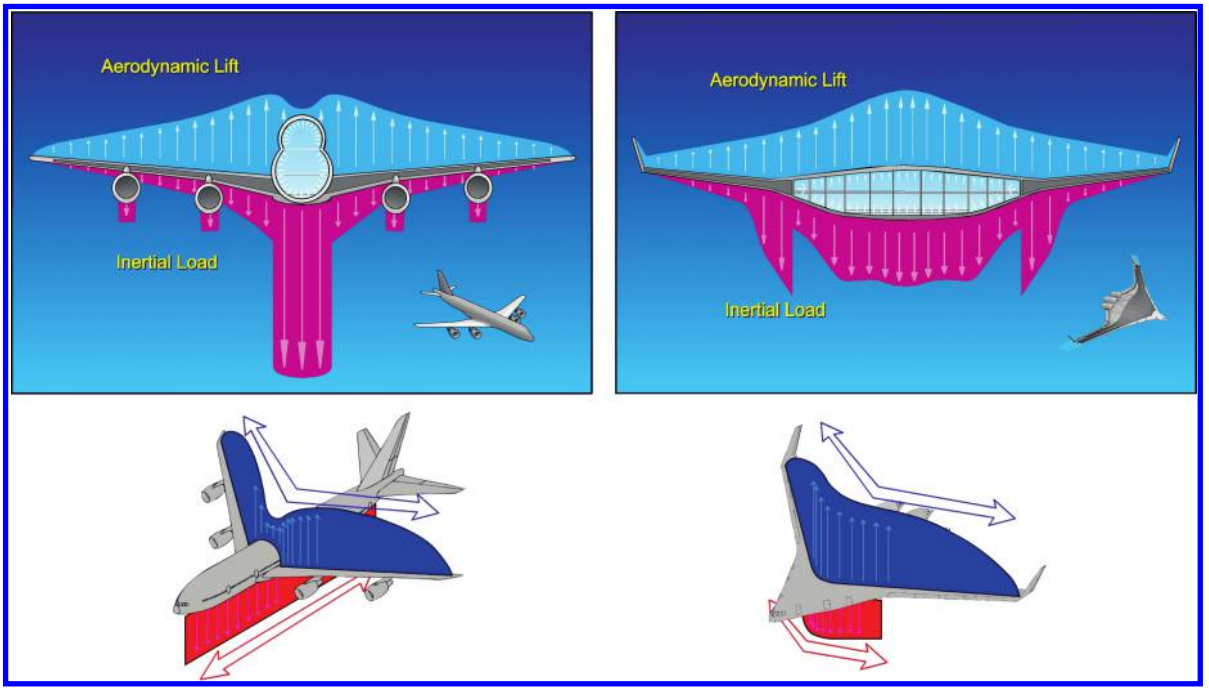

Fig. 19 Comparison of aerodynamic, inertial, and cabin pressure loads.

F. Propulsion

The aft engine location on the BWB offers the opportunity for ingestion of the boundary layer generated on the centerbody forward of the inlets. In principle, boundary-layer ingestion (BLI) can improve the propulsive efficiency by reducing ram drag. This assumes that an inlet can be designed that provides proper pressure recovery and uniform flow at the fan face of the engine. Alternatively, the boundary layer can be diverted around the sides of the inlets, but this implies dumping low-energy air into an already transonically stressed pressure recovery region. Simply mounting the engines on pylons is another option, but increased wetted area and weight plus nosedown thrust moment are detractors from this installation.

NASA-sponsored studies of the BLI concept were conducted at the University of Southern California (USC) and at Stanford University. At USC, a wind-tunnel simulation was created with an upstream flat plate to generate the boundary layer and various duct geometries, leading to a station representing the fan face of the engine, where the flow quality was evaluated. Results indicated that proper configurations of vortex generators could provide a reasonably uniform flow at the fan face with acceptable pressure recovery. These results were utilized at Stanford University to help guide a theoretical multidisciplinary optimization study of the BWB engine inlet concept. Navier–Stokes based CFD was used to represent the centerbody and inlet flowfield, and engine performance was modeled as a function of the flow quality at the fan face. The optimizer indicated that minimum fuel burn was obtained with the engine swallowing the boundary layer, as opposed to diverting the boundary layer around the inlet.[4,5]

The aft engine location of the BWB allows for several installation options; however, integration affects all of the basic disciplines. Uniquely for a BWB, there is no explicit penalty for the centerline engine of a three-engine installation. Candidate installation concepts include podded with pylon, upper or lower surface inlet with S-duct, BLI, or diverter; and, finally, the engine count itself. Airplanes were sized for 12 different combinations with appropriate gains and losses for inlet recovery and distortion, wetted area drag (including the adjustment for BLI), weight, and thrust moment. The figure of merit was the TOGW. Additional considerations included ditching, emergency egress, foreign object damage (FOD), noise, reverse thrust, and maintainability. Lower surface inlets were discarded on the basis of FOD and ditching. A three-engine configuration with upper surface BLI inlets and S-ducts to the engines was selected. If BLI did not prove practical, boundary-layer diverters were assumed to be the default.

G. Structure

The unique element of the BWB structure is the centerbody. As the passenger cabin, it must carry the pressure load in bending, and as a wing it must carry the wing bending load. A comparison of the structural loading of a BWB with that of a conventional configuration is given in Fig. 19. Peak wing bending moment and shear for the BWB is on the order of one-half of that of the conventional configuration. The primary challenge was to develop a centerbody structural concept to absorb the cabin pressure load. Unlike a wing, which rarely experiences its design load (typically via a 2.5-g gust), the passenger cabin sees its design pressure load on every flight. Thus, on the basis of fatigue alone, the centerbody should be built from composites due to their comparative immunity to fatigue.

The overall structural concept selected for this NASA-sponsored study is shown in Fig. 20. Outboard wing structure is essentially conventional and was assumed to be composite. The centerbody structural shell was based on two candidate concepts: a 5-in. thick sandwich, or a skin plus 5-in. deep hat-section stringers. A global finite element model was analyzed for the combined pressure and wing bending loads on the centerbody. Cabin skin deflection due to a two times pressure load is shown in Fig. 21.

H. Safety and Environmental

The BWB offers several inherent safety features that are unique to the configuration. An uncontained engine failure can not impact the pressure vessel, fuel tanks, or systems. The pressure vessel itself is unusually robust because its structure has been sized to carry both the pressure loads and wing bending loads, and, consequently, its crashworthiness should be substantial.

Environmentally, the BWB naturally offers a low acoustic signature, before any specific acoustic treatment. The centerbody shields forward radiated fan nose, and engine exhaust noise is not reflected from the lower surface of the wing. Airframe noise is reduced by the absence of a slotted flap trailing-edge high-lift system. Engine emissions are reduced in direct proportion to the reduced fuel burn per seat mile described hereafter.

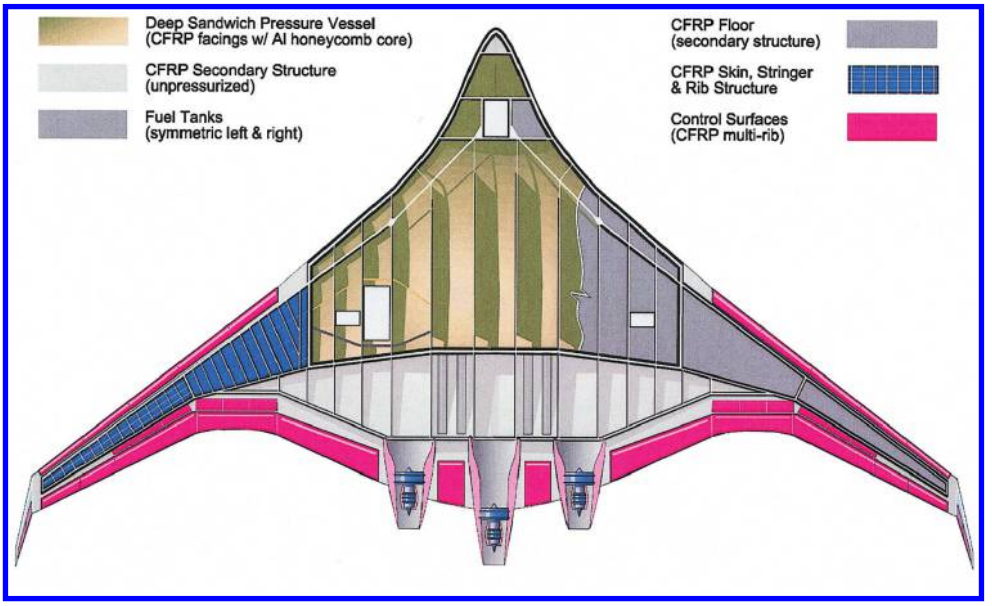

Fig. 20 Structural layout of second-generation BWB.

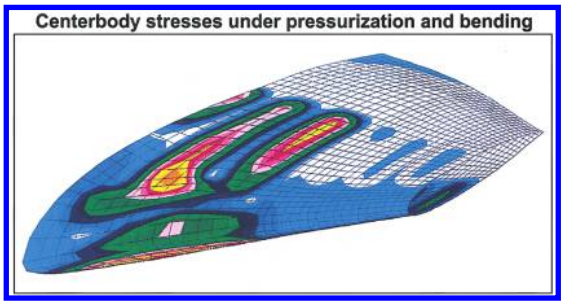

Fig. 21 Finite element model solution showing exaggerated cabin skin deflection at two times pressure.

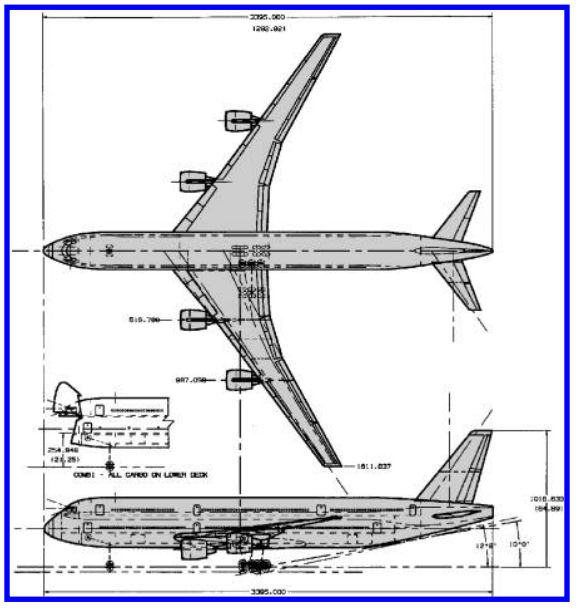

Fig. 22 Conventional baseline configuration.

I. Performance

A proper evaluation of the BWB concept required that a conventional subsonic transport be sized to the same design mission, employing the same composite structure technology and the same class of advanced technology engines. A two-view of the conventional baseline is shown in Fig. 22, and Table 1 compares the performance of the BWB with the baseline. In addition to the significant reduction in weight, the BWB requires one less 60,000-lb-class engine, and its fuel burn per seat mile is 27% lower. Given that the configuration was the only technical difference in these two airplanes, the potential for the BWB concept was regarded as remarkable.

Table 1 Performance comparison of the second-generation BWB with the conventional baseline airplane

Model	BWB	Conventional
Passengers	800	800
Range, n mile	7,000	7,000
MTOGW, lb	823,000	970,000
OEW, lb	412,000	470,000
Fuel burned, lb	213,000	294,000
L/D at cruise	23	19
Thrust, total lb	$3 \times 61{,}600$	$4 \times 63{,}600$

Table 2 Design requirements and objectives for the Boeing BWB-450 baseline

Parameter	Value
Payload	468 passengers + baggage, three-class arrangement
Design range	7750 n mile
Crew	Standard two-man crew
Reserves	International reserve fuel Fuel equal to 5% of block fuel 200 n mile diversion to alternate airport One-half hour hold at 1500 ft at holding speed
Constraints	11,000-ft field length 140-kn approach speed 2.7° segment climb gradient 300-ft/min excess power at top of climb

V. Boeing BWB-450 Baseline Airplane

The three-year study just described demonstrated the feasibility and performance potential of the BWB. Based on these results and predictions, it was decided to initiate a Boeing preliminary design study of a BWB transport. The 800-passenger 7000-n mile design mission of the feasibility studies was deemed inappropriate for the in-house evaluation of the BWB. Comparisons with existing airplanes and airplanes of other preliminary design studies would not be possible, and a payload of 800 passengers was simply beyond market forecast data.

A. Design Requirements and Objectives

The design mission selected for the baseline BWB is given in Table 2. Although distinct from existing airplanes, this specification

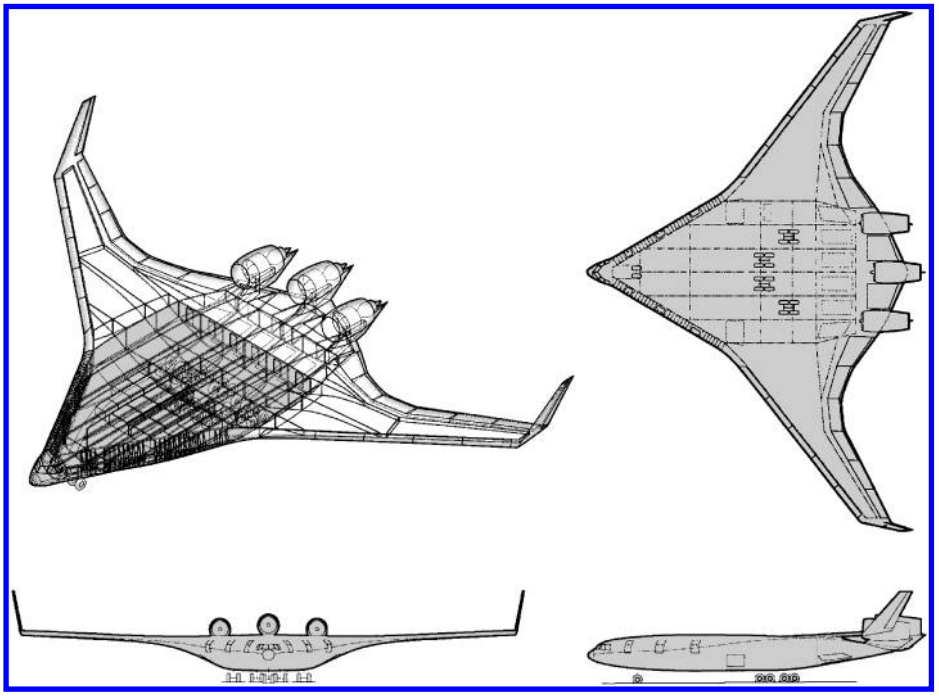

Fig. 23 Boeing BWB-450 baseline.

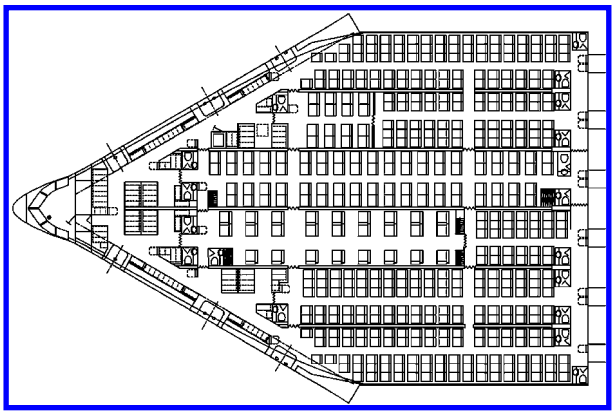

Fig. 24 Three-class interior arrangement.

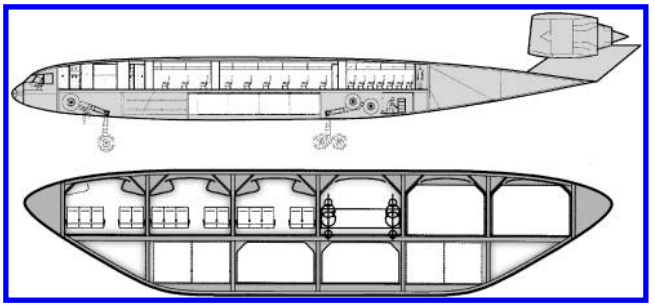

Fig. 25 Centerbody interior cross sections.

offered the opportunity for some comparison of the resulting BWB with the B747, A340, and the then-pending A3XX. Initial specification of 450 passengers (hence, the designation BWB-450) was considered nominal, and the final passenger count would be established as the airplane was configured and sized. Also, although somewhat ignored in the earlier studies, airport compatibility requirements were enforced for the baseline BWB, in particular, the wingspan limit of 262 ft (80 m).

B. Configuration of the Boeing BWB-450 Baseline

Per the requirements just listed and the optimization procedure described hereafter, the baseline BWB shown in Fig. 23 was created. Minimum TOGW was the objective function. Trapezoidal aspect ratio is 7.55, down substantially from the earlier BWBs, and the wingspan of 249 ft fits easily within the 80-m box for Class VI airports. Passenger count is 478, based on three-class international rules. Figure 24 shows the interior arrangement, and Fig. 25 shows representative cross sections of the centerbody. The entire passenger cabin is on the upper deck, and cargo is carried on the lower deck, similar to conventional transports. All of the payload is located ahead of the rear spar. Crashworthiness contributed to this arrangement.

C. Multidisciplinary Design Optimization

As described, the BWB is an integrated configuration where the interaction of the basic disciplines is unusually strong. Conventional design intuition and approach are challenged, if not overwhelmed, when faced with sizing and optimizing the BWB airplane. The method of Ref. 6, a pragmatic and functional multidisciplinary airplane design optimization code, was adopted. This work has evolved into a Boeing proprietary code called WingMOD. In the case of the BWB, the airplane is defined by an initial planform and a stack of airfoils whose section characteristics, for example, moment coefficient c_{mac} and drag coefficient c_d, are known as a function of thickness-to-chord ratio t/c, section lift coefficient c_l and Mach number. WingMOD then models the airplane with a vortex–lattice code and monocoque beam analysis, coupled to give static aeroelastic loads. The model is trimmed at several flight conditions to obtain load and induced drag data. Profile and compressibility drag are then evaluated at stations across the span, based on the airfoil section properties and the vortex–lattice solution. Structural weight is calculated from the maximum elastic loads encountered through a range of flight conditions, including maneuver and vertical and lateral gusts. The structure is sized based on bending strength and buckling stability considerations. Maximum lift is evaluated by the use of a critical section method that declares the wing to be at its maximum useable lift when any spanwise airfoil section reaches its maximum lift coefficient.

Figure 26 shows a small portion of an example WingMOD solution for the baseline BWB-450. The procedure begins with the manual definition of a baseline design (not to be confused with the

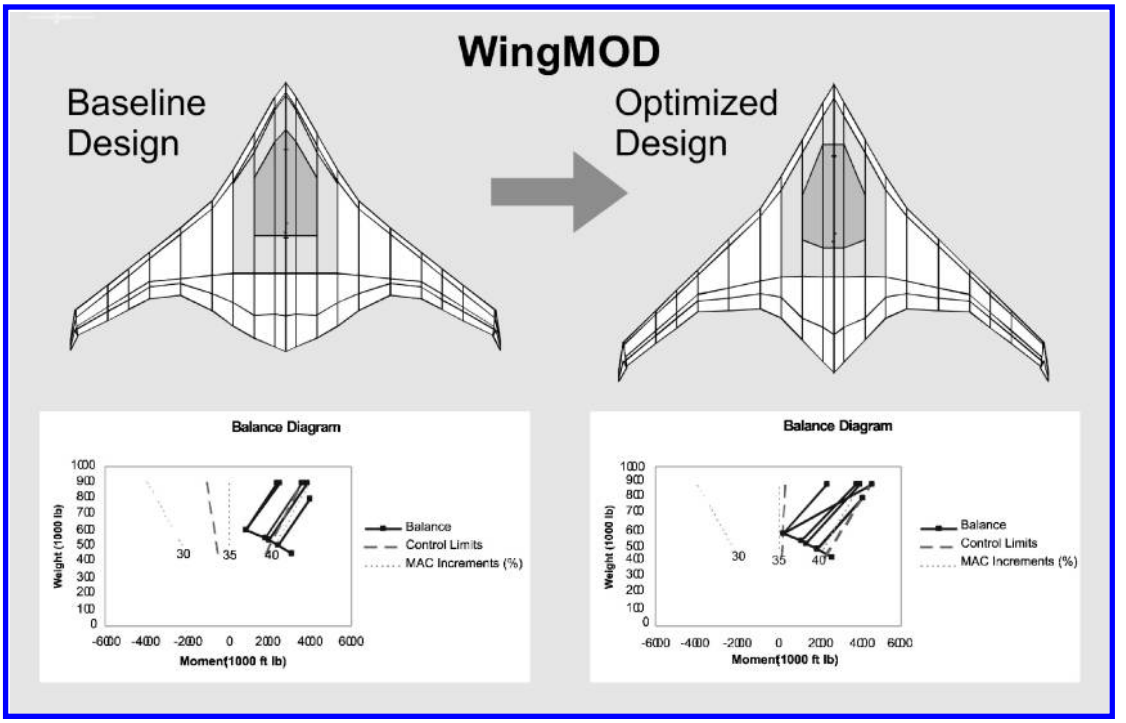

Fig. 26 Example WingMOD solution for the BWB baseline.

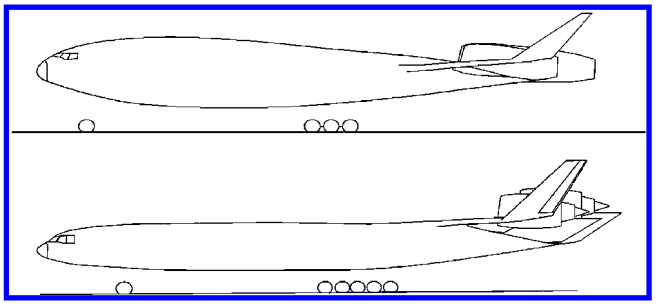

Fig. 27 Comparison of centerbody profiles of the second-generation BWB with the Boeing baseline BWB.

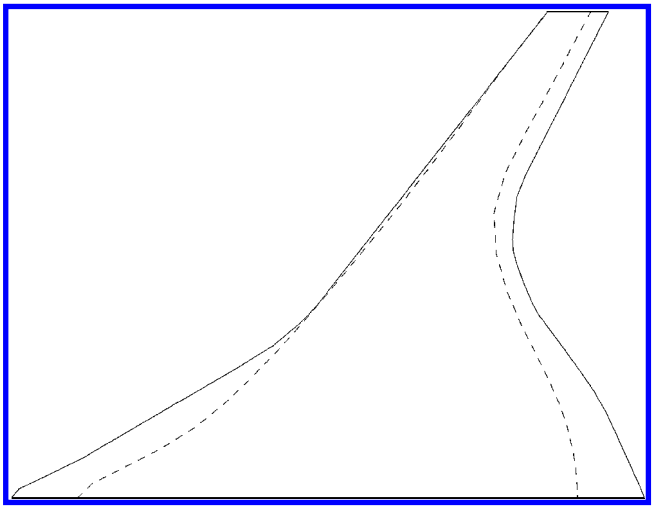

Fig. 28 Planform comparisons of the second-generation BWB with the Boeing Baseline BWB: ——, Boeing Baseline and – – –, second generation (scaled).

term "baseline BWB"). Subject to the mission definition and constraints (e.g., range, takeoff field length, approach speed, interior volume, etc.), WingMOD provides the definition of the minimum TOGW configuration that meets the mission while satisfying all constraints. Put another way, the optimized airplane design is closed and meets all design mission requirements with minimum TOGW.

D. Aerodynamics

Aerodynamic design of the BWB-450 was coupled with WingMOD to obtain the final aerodynamic definition (outer mold line). Definition of the airfoil stack was a key element to this approach. A new class of transonic airfoils for the centerbody was designed based on constraints of cross-sectional area required to hold passengers, baggage, and cargo properly. The new airfoils tightly package the payload without a drag penalty. More significantly, the new airfoils smoothed and flattened the geometry to simplify manufacture. Figure 27 shows a comparison of the centerbody profile of the second-generation BWB with the Boeing BWB-450.

The planform also underwent significant change from the second-generation BWB, as shown in Fig. 28, which also gives the comparison where both planforms are scaled to the same wingspan. Airfoil chords have been increased on both the outer wing and the centerbody. Buffet onset level and characteristics primarily drove outboard chord increase. Figure 29 compares the lift curves (C_L vs α) and lift vs pitching moment curves (C_L vs C_M) for the BWB-450 and the second-generation BWB. If the buffet C_L is defined at the break in the C_L vs C_M curve, the improvement of the new planform is apparent. Compared to the earlier design, there is almost twice the margin between midcruise C_L, 1.3 g–buffet, and buffet itself. Centerbody chords were increased to reduce their thickness-to-chord and afterbody closure angles. Although this increased wetted area, the increased friction drag was more than offset by a reduction in pressure drag. Inboard elevon effectiveness was also improved. Aerodynamic design of the BWB is discussed in more detail in Ref. 7.

E. Stability and Control

The planform, airfoil stack, and twist distribution of the BWB-450 resolves the longitudinal trim problem with more efficiency than most flying-wing airplanes. Historically, flying wings have been trimmed by sweeping the wing and downloading the wingtips. Whereas this approach allows the wingtips to functionally serve as a

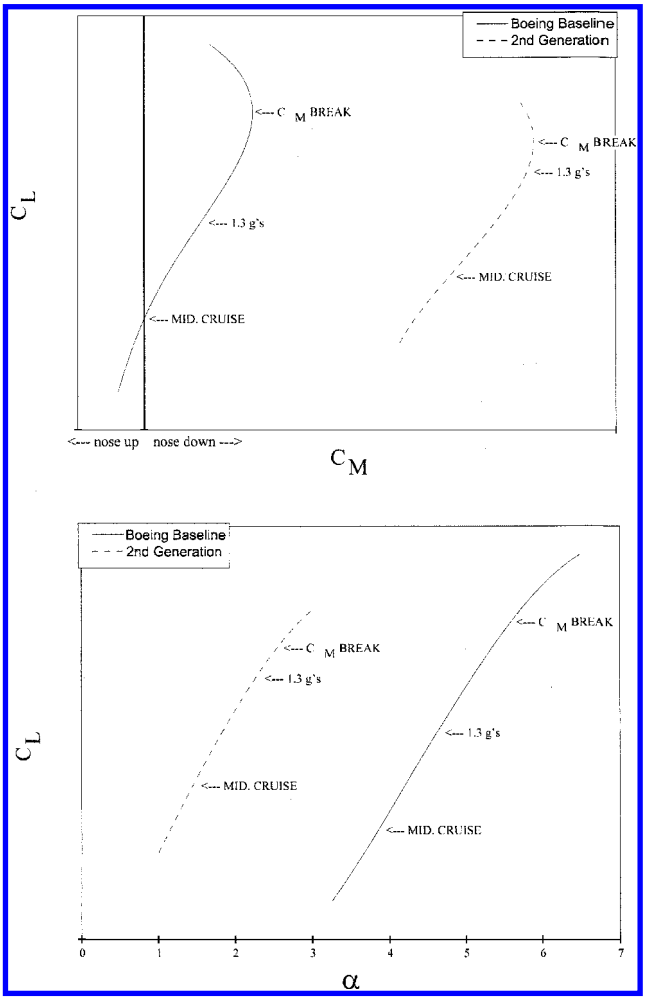

Fig. 29 Comparison of lift and moment curves of the second-generation BWB with the Boeing Baseline BWB.

horizontal tail, it imposes a significant induced drag penalty. The effective aerodynamic wingspan is less than the physical span, and this penalty is a primary reason that flying-wing airplanes have failed to live up to their performance potential. As described earlier, the first- and second-generation BWB were allowed to have significantly negative static margins to preserve a near-elliptic spanload. The BWB-450 has been trimmed by a careful distribution of spanload coupled with a judicious application of wing washout. The result is a flying-wing airplane that is trimmed at a stable center of gravity (+5% static margin) with all control surfaces faired, and with no induced drag penalty. Setting this design condition at the midcruise point results in a trim drag of one count at start of cruise (high C_L), and a one-half count of trim drag at end of cruise (lower C_L).

F. Propulsion

The second-generation BWB assumed boundary-layer ingestion for both the engine installation and the performance estimate. For the BWB-450 it was decided to reduce the technology risk by examining the performance of both boundary-layer diverters and simple podded engines on pylons. Navier–Stokes based CFD was used to evaluate these options. To the extent they were studied, the diverters showed an unacceptable drag increase due to the low energy of the diverted boundary layer, plus its interaction with the pressure recovery region of the aft centerbody. Alternatively, the initial modeling of the podded engines on pylons indicated that the increase in wetted area was only 4% compared to the diverted configuration. The thrust moment, although undesirable, was deemed acceptable. A thorough CFD-based design and analysis study showed that an interference-free podded engine and pylon installation could be achieved, and the net drag penalty was simply due to the wetted area increase. Therefore, podded engines on pylons became the selected installation for the baseline BWB.

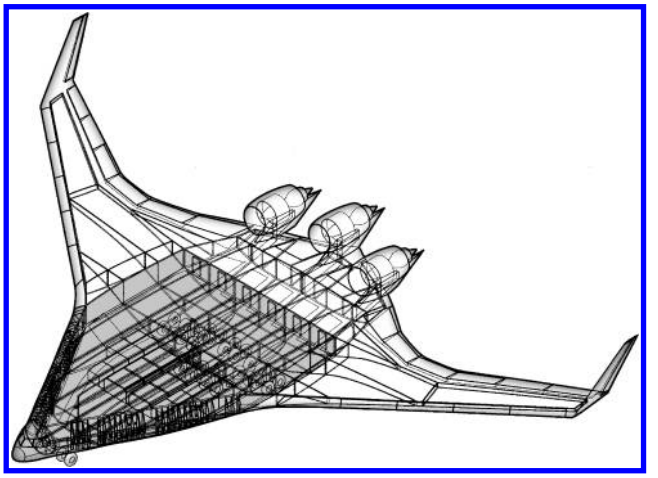

Fig. 30 Centerbody structural concept.

G. Structure

The BWB structure is divided into two main components: the centerbody and the outer wings. The structure of the outer wings is similar to that of a conventional transport. The centerbody is subdivided into the forward pressure vessel and the unpressurized afterbody. Development of the structure for the centerbody and its pressure vessel was approached by defining and comparing several concepts. Weight and cost were the primary figures of merit. One of the most viable concepts was based on a skin/stringer outer surface structure where the stringers are on the order of 5–6 in. deep. The internal ribs have *Y* braces where they meet the skin, to reduce the bending moment on the skin created by the internal pressure. (This could be regarded as a structural analog to the earlier concept of an arched pressure membrane.) As shown in Fig. 30, the complete centerbody pressure vessel is composed of the upper and lower surface panels, the rounded leading edge (which also functions as the front spar), the rear main spar, the outer ribs (which must also carry the cabin pressure load in bending), and the internal ribs (which carry the cabin pressure load in tension). The cabin floor simply supports the payload and does not carry wing bending loads. Finite element analyses have been used to develop and verify this structural concept and its weight. The final result is an unusually rugged passenger cabin that weighs little more than a conventional fuselage.

Studies to date have assumed composite material for the majority of the BWB primary structure. The outer wings could readily be fabricated from aluminum with the typical 20% weight penalty. However, as mentioned earlier, the weight penalty for using aluminum for the centerbody structure would be larger. The design cabin pressure load is experienced on every flight, and, thus, fatigue becomes the design condition. Because cabin pressure loads are taken in bending, the margin required for aluminum could be prohibitive, whereas composites are essentially immune to fatigue and, hence, would suffer no penalty.

Figure 31 shows a comparison of the structural weight fractions of a BWB and a conventional configuration, both sized for the same mission and both assuming the same composite structure technology. Although the centerbody structure of the BWB is heavier than that of a conventional fuselage, the weight (OEW) of the complete configuration of the BWB is markedly lighter.

H. Performance

A performance comparison of the Boeing BWB-450 with the Airbus A380-700 is given in Fig. 32. Both airplanes are compared for a payload of approximately 480 passengers and a range of 8700 n mile. (A380 data are from an Airbus brochure.) Probably the most striking result is the BWB's 32% lower fuel burn per seat.

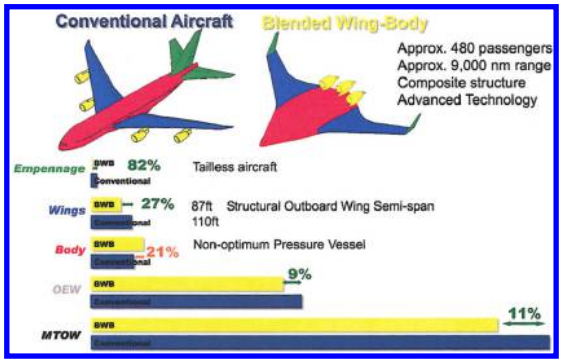

Fig. 31 Comparison of structural weight fractions from a BWB and a conventional configuration.

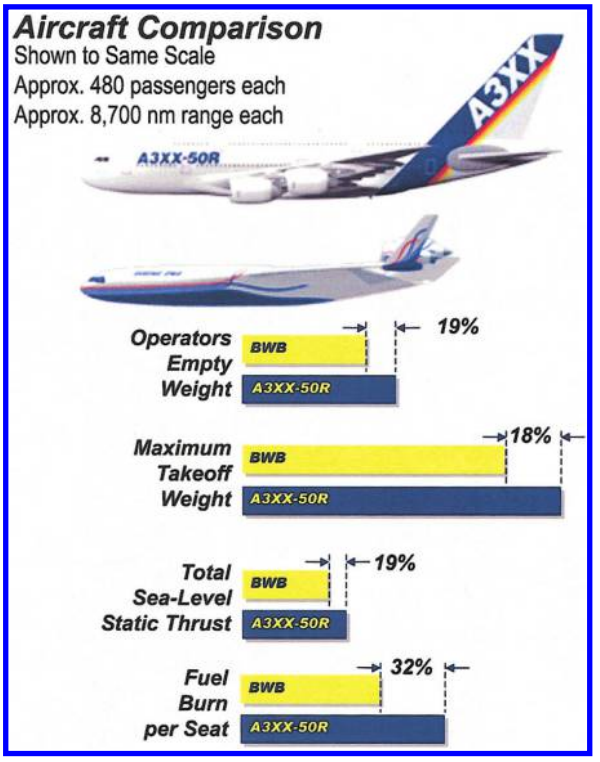

Fig. 32 Performance comparison of the BWB-450 with the A380-700.

Both airplanes are using equivalent technology engines of similar thrust levels; however, the A380-700 requires four, whereas the BWB-450 requires three. The primary structure of the A380-700 is aluminum, with the exception of the outer wing panels, which are understood to be composite. The BWB-450 primary structure is essentially all composite. A comparison of the BWB-450 cabin volume with that of the A380-700 is shown in Fig. 33.

I. Environment

The Boeing BWB-450 offers the potential for a significant reduction in environmental emissions and noise. Lower total installed thrust and lower fuel burn imply an equivalent reduction in engine emissions, under the assumption of the same engine technology. As discussed earlier, the forward-radiated fan noise is shielded by the vast centerbody, and engine exhaust noise is not reflected by the lower surface of the wing. The lower thrust loading itself implies lower noise. There are no slotted trailing-edge flaps, so a major source of airframe noise is eliminated. Thus, before any specific acoustic treatment, the BWB offers a significant reduction in noise.

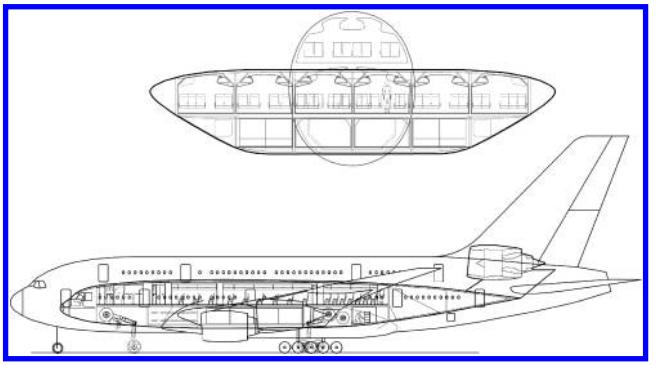

Fig. 33 Interior volume comparison of the BWB-450 with the A380-700.

VI. Unique Opportunities and Challenges of the BWB Configuration

Creation of the original BWB was motivated by a search for an airplane configuration that could offer improved efficiency over the classic tube and wing. Takeoff weight and fuel burn were the primary figures of merit, and the BWB concept has shown substantial reductions in these two performance parameters, as described earlier. However, the BWB configuration offers some unique opportunities that were neither envisioned nor planned during its original creation in 1993. Three of these are described hereafter.

A. Manufacturing Part Count

The BWB is simply a big wing with an integrated fuselage and no empennage, save the winglets/verticals. There are no complex wing–fuselage and fuselage–empennage joints of highly loaded structures at 90 deg to one another, and there are no fillets. All trailing-edge control surfaces are simple hinged with no track motion, and there are no spoilers. This manifests a substantial reduction (on the order of 30%) in the number of parts when compared to a conventional configuration. A similar reduction in manufacturing recurring cost is implied.

B. Family and Growth

Reference 2, which describes the early development of the BWB, contains the remark; "Any change such as wing area or cabin volume implies a complete reconfiguration. Stretching is not in the vocabulary." That was the thought at the time. As development progressed, it was discovered that the BWB concept could be ideal for a family of airplanes with the potential for substantial commonality among its members. Here stretching takes place laterally (spanwise), as opposed to longitudinally. Passenger capacity can be increased by adding a central bay to the centerbody and vice versa. Wing area and span automatically increase or decrease appropriately with passenger capacity, a quality not offered by the longitudinal stretching of a conventional airplane.

To achieve this growth capability, the aerodynamic outer mold lines of all of the family members must remain smooth and provide proper aerodynamic performance. In addition, all of the airplanes must be trimmed and balanced. Geometrically, this has been achieved by essentially defining the centerbody as a ruled surface in the spanwise direction. In turn, this allows the definition of several airplanes ranging, for example, from 250 to 550 passengers, as shown in Fig. 34. Centerbody cabins are composed of combinations of two or more distinct cabins (shown in green, yellow, and orange). The outer wing panels and nose sections (shown in blue) are of identical geometry for all family members. Distinct to each airplane are the transition section aft of the nose, the aft centerbody, and engines (shown in gray). Nose gear and outer main gear could be common for all family members, with a center main gear of varying capacity added where required.

A representative set of the airplane family has been examined in depth to establish the potential for commonality. A common part number for the entire outer wing was the goal. Fuel volume of the outer wing is adequate for all members of the family. Navier–Stokes

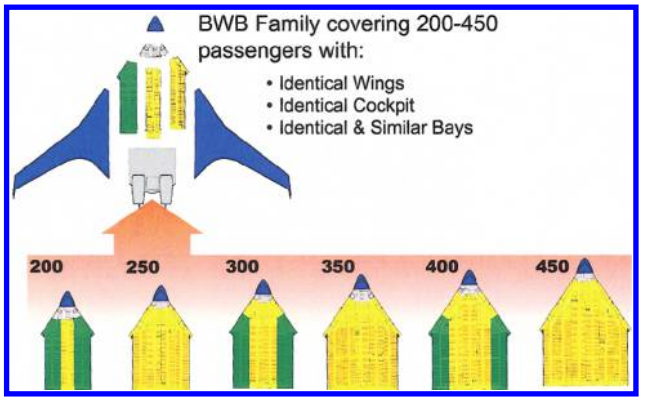

Fig. 34 Commonality of a BWB family.

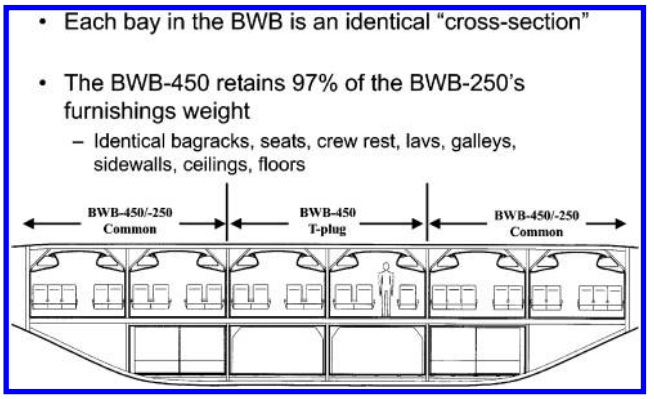

Fig. 35 Cabin cross-sectional growth from 250 to 450 passengers.

analyses of several of the members of this example family demonstrated proper aerodynamic performance. The airplanes are trimmed and balanced. Finite element modeling was used to quantify the effect of commonality on the structure. The proposed commonality was feasible, but at a cost of increased OEW for the smaller airplanes. If the common part number requirement is relaxed to permit a skin gauge change, the OEW penalty is substantially reduced.

Commonality extends naturally to the interior, once the commitment to the centerbody growth concept is made. In principle, the cabin cross section is the same for all of the airplanes, as shown in Fig. 35. This implies common galleys, lavatories, bag racks, and seats. Substantial maintenance and life-cycle cost savings are implied for the airline customer.

Put simply, commonality is a constraint, and almost any constraint imposed on an airplane is manifested by an increase in weight. However, the BWB concept appears to offer the opportunity for an unusual level of commonality while the aerodynamic efficiency is maintained via the natural variation of wing area and span with weight. This implies significant reductions in part count and learning curve penalties in manufacturing. Enhanced responsiveness to fleet-mix requirements is also implied. It remains to evaluate thoroughly the trade between airplane cost and performance offered by the BWB family concept.

C. Speed

Figure 36 shows a comparison of the BWB-450 cross-sectional area variation $S(x)$ with that of the classical minimum wave drag due to the volume of the Sears–Haak body. Also shown is the variation for an MD-11. It can be observed that the BWB is naturally area-ruled, and, hence, a higher cruise Mach number should be achievable without a change in the basic configuration geometry. Figure 37 gives the results of a WingMOD-based study for the effect of the design cruise Mach number on BWB performance and weight. All of the designs are closed, trimmed, and balanced for the same design mission. Variation between planforms appears slight; however, a comparison between the $M = 0.85$ and 0.95 designs shows a significant distinction. Increased Mach number is accommodated by an increase in sweep and chord, which results in a corresponding increase in weight. Some of this weight increase is due to the increase of installed engine SFC with Mach number. The classic aerodynamic parameter ML/D is plotted as a function of the cruise Mach number in Fig. 37. A more meaningful graph is given by the variation of the parameter MP/D, also shown in Fig. 37. (P is the design payload weight.) MP/D includes the effect of airplane weight itself, because $MP/D = (ML/D) \times (P/W)$. Isometric views of BWBs designed for $M = 0.85$, 0.90 and 0.95 are given in Fig. 38.

These preliminary results suggest that 0.90 could be the best cruise Mach number. However, the economic value of speed must be established before selecting a design cruise Mach number. For example, airplane utilization varies directly with speed, and for some

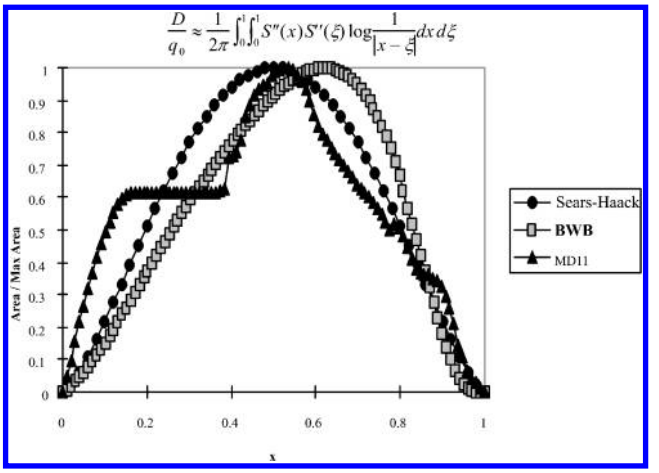

Fig. 36 Cross-sectional area variations, $S_{(x)}$ vs x.

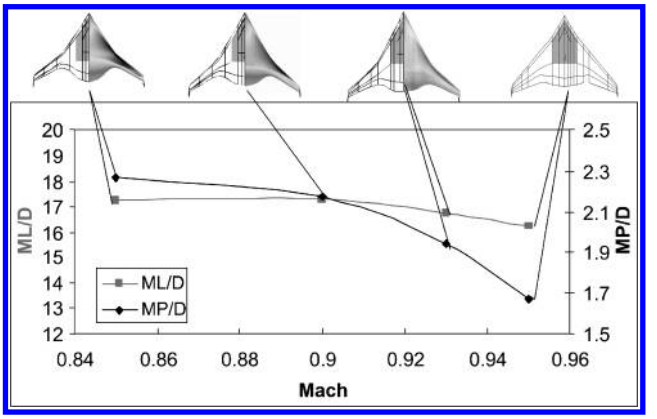

Fig. 37 BWB planform, *ML/D* and *MP/D* variation with Mach number.

Fig. 38 Comparison of BWB-250 configuration with Mach number.

longer-range missions, a slight increase in speed could eliminate the requirement for a second crew. The question then becomes, how much of an increase in TOGW and fuel burn can be offset by such issues? Resolution remains to be found.

D. Passenger Acceptance, Ride Quality, and Emergency Egress

The unique interior configuration of the BWB offers both opportunities and challenges. Vertical walls of the passenger cabins provide a more spacious environment, similar to a railroad car rather than the curved walls of a conventional airplane. At the same time, the low capacity of each cabin (approximately 100 passengers) provides an intimacy not available in wide-body conventional transports. However, although there is a window in each main cabin door, there are no windows in the cabin walls. As a surrogate for windows, a flat screen display connected to an array of digital video cameras will make every seat a window seat. Some example interior renderings are shown in Fig. 39.

Ride quality has been a concern due to the lateral offset of the passengers from the center of gravity. This has been addressed by comparison of the results from piloted flight simulator tests of the BWB-450 and a B747-400 using the same pilots and flight profile. One of the more severe cases studied was a takeoff, go-around, and landing in moderate turbulence with a 35-kn crosswind. Lateral and vertical rms g levels were comparable for the "worst" seats in both airplanes; however, the frequency content tended to be lower for the BWB. Gust load alleviation was not used on either airplane.

Emergency egress becomes a significant challenge when passenger capacity exceeds 400. This is simply a consequence of the square-cube law: Capacity increases with the cube of the length scale, whereas surface area for egress increases with the square of the length scale. The BWB configuration lends itself particularly well to resolving this problem. There is a main cabin door directly in the front of each aisle, and an emergency exit through the aft pressure bulkhead at the back of each aisle. In addition, there are four cross aisles, as shown in Fig. 40.

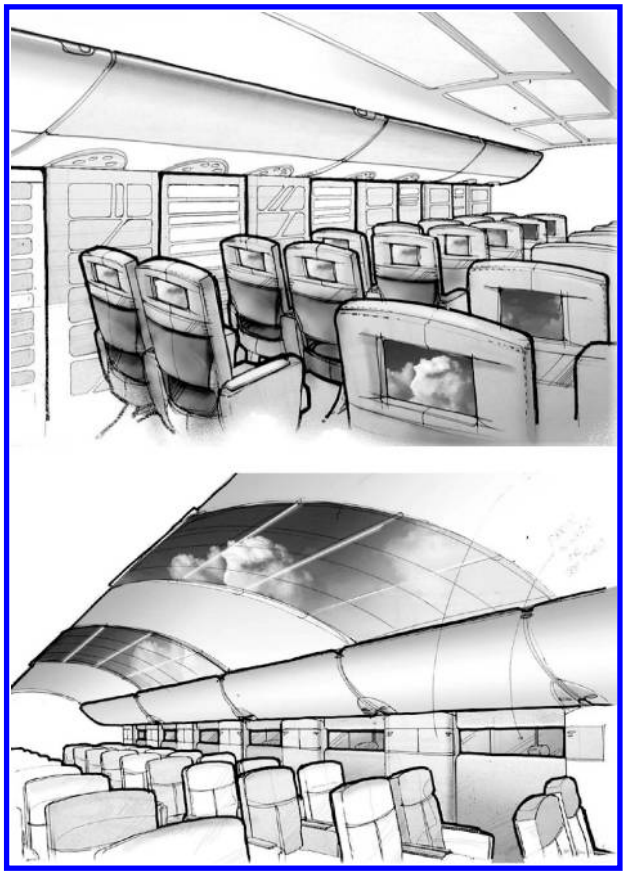

Fig. 39 Interior concepts for the BWB.

Table 3 Issues and areas of risk (from Douglas Aircraft Co., 1955)

• Complex flight control architecture and allocation, with sever hydraulic requirements
• Large auxiliary power requirements
• New class of engine installation
• Flight behavior beyond stall
• High floor angle on take off and approach to landing
• Acceptance by the flying public
• Performance at long range
• Experience and data base for new class of configuration limited to military aircraft

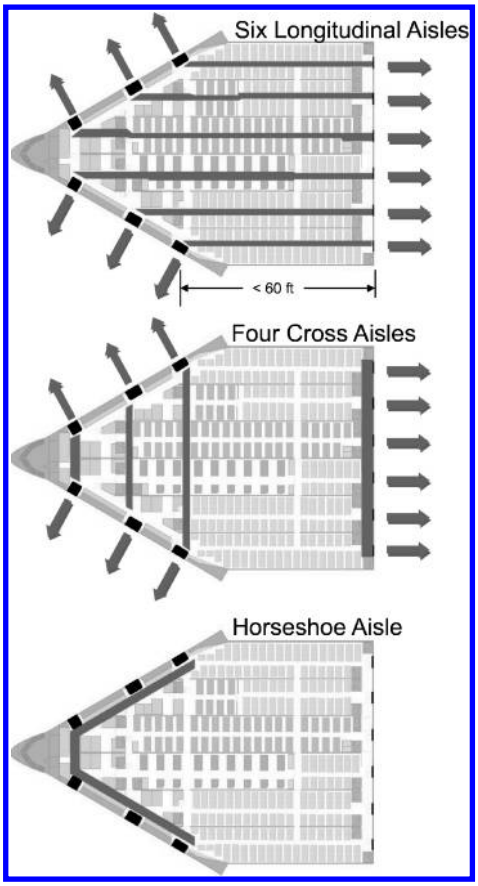

Fig. 40 Cabin egress flow patterns.

Thus, from virtually any location in the cabin, a passenger will have a direct view of one or more exits. Unlike a conventional transport, a 90-deg turn will not be required to reach a door from the aisle. Because there is no upper deck, the problems with long slides, slide interference, and overwing exits do not exist. Ultimately, this new class of interior configuration will require a new set of emergency evacuation criteria coordinated with the Federal Aviation Administration.

VII. Summary

Development of the BWB has progressed steadily over the past seven years. Once-apparent "show-stoppers" have been reduced to technical challenges, or, in most cases, proper solutions. From a distance, the Boeing BWB-450 baseline airplane shows little distinction from the first-generation BWB developed under NASA sponsorship in 1993. The intent of this paper has been to chronicle the engineering work that has brought the airplane to the state it is in today. Table 3 presents a list of issues and areas of risk. They could readily apply to the BWB. However, they are, in fact, extracted from Douglas Aircraft Company memoranda written in the 1950s regarding the challenge of moving from the DC-7 to the DC-8. Hopefully, our industry will press on, just as Douglas and Boeing did 50 years ago.

Acknowledgments

The creation and initial development of the Blended-Wing–Body (BWB) concept was stimulated and funded by NASA Langley Research Center, primarily under contract NAS1-20275. NASA involvement with the BWB has continued with their design and fabrication of the BWB Low-Speed Vehicle flight demonstrator. NASA's initiative and involvement with the BWB has been critical to the success of the concept. Their participation is gratefully acknowledged. The BWB exists today because of the contributions of an array of very special engineers. Following is a partial list (partial, because it seems inevitable that a key individual will have been overlooked) of those whose contributions have been fundamental to the development of the BWB: John Allen, Amer Anabtawi, Robert Bird, Ron Blackwelder, Derrell Brown, George Busby, Jerry Callaghan, Peter Camacho, Douglas Cameron, Louis Feiner, Douglas Friedman, Ronald Fox, Richard Gilmore, Raquel Girvin, Antonio Gonzales, Arthur Hawley, Ronald Kawai, Ilan Kroo, David Kwok, Peter Lissaman, Roger Lyon, Jacob Markish, Robert McKinley, Mark Meyer, Joshua Nelson, Alan Okazaki, Wayne Oliver, Mark Page, Dhar Patel, Wilfred Pearce, Regina Pelkman, Chris Porter, Mark Potsdam, Norman Princen, Blaine Rawdon, Melvin Rice, William Rickard, David Rodriguez, Dino Roman, Kevin Roughen, George Rowland, Peter Rumsey, Debbie Runyan, Matt Salcius, Paul Scott, Robert Seplak, Leonel Serrano, William Small, Norbert Smith, Darrel Tenney, Ben Tigner, William Vargo, Sean Wakayama, William Watson, Jennifer Whitlock, Matthew Wilks, Karen Willcox, Kenneth Williams.

References

[1]Liebeck, R. H., "Design of Subsonic Airfoils for High Lift," *Journal of Aircraft*, Vol. 15, Sept. 1978, pp. 549–561.

[2]Liebeck, R. H., Page, M. A., Rawdon, B. K., Scott, P. W., and Wright, R. A., "Concepts for Advanced Subsonic Transports," NASA CR 4624, Sept. 1994.

[3]Liebeck, R. H., Page, M. A., and Rawdon, B. K., "Blended-Wing-Body Subsonic Commercial Transport," AIAA Paper 98-0438, Jan. 1998.

[4]Anabtawi, A., "Experimental Investigation of Boundary Layer Ingestion into Diffusing Inlets," Ph.D. Dissertation, Aerospace Engineering Dept., Univ. of Southern California, Aug. 1999.

[5]Rodriguez, D. L., "A Multidisciplinary Optimization Method for Designing Boundary Layer Ingesting Inlets," Ph.D. Dissertation, Dept. of Aeronautics and Astronautics, Stanford Univ., Stanford, CA, Jan. 2001.

[6]Wakayama, S., "Blended-Wing-Body Optimization Problem Setup," AIAA Paper 2000-4740, Sept. 2000.

[7]Roman, D., Allen, J. B., and Liebeck, R. H., "Aerodynamic Design of the Blended-Wing-Body Subsonic Transport," AIAA Paper 2000-4335, Aug. 2000.

This article has been cited by:

1. Albert S.J. van Heerden, Marin D. Guenov, Arturo Molina-Cristóbal. 2019. Evolvability and design reuse in civil jet transport aircraft. *Progress in Aerospace Sciences* **108**, 121-155. [Crossref]
2. Hyunmin Choi, Jinsoo Cho. 2019. Aerodynamic Analysis and Parametric Study of the Blended-Wing-Body-Type Business Jet. *International Journal of Aeronautical and Space Sciences* **20**:2, 335-345. [Crossref]
3. Mohammed Ba Zuhair. 2019. BALANCING AN AIRCRAFT WITH SYMMETRICALLY DEFLECTED SPLIT ELEVATOR AND RUDDER DURING SHORT LANDING RUN. *Aviation* **23**:1, 23-30. [Crossref]
4. Wensheng Zhu, Xiongqing Yu, Yu Wang. 2019. Layout Optimization for Blended Wing Body Aircraft Structure. *International Journal of Aeronautical and Space Sciences* **41**. . [Crossref]
5. Gang Yu, Dong Li, Yue Shu, Zeyu Zhang. 2019. Numerical Simulation for Engine/Airframe Interaction Effects of the BWB300 on Aerodynamic Performances. *International Journal of Aerospace Engineering* **2019**, 1-15. [Crossref]
6. Nicholas B Cramer, Daniel W Cellucci, Olivia B Formoso, Christine E Gregg, Benjamin E Jenett, Joseph H Kim, Martynas Lendraitis, Sean S Swei, Greenfield T Trinh, Khanh V Trinh, Kenneth C Cheung. 2019. Elastic shape morphing of ultralight structures by programmable assembly. *Smart Materials and Structures* **28**:5, 055006. [Crossref]
7. Dominic Keidel, Giulio Molinari, Paolo Ermanni. 2019. Aero-structural optimization and analysis of a camber-morphing flying wing: Structural and wind tunnel testing. *Journal of Intelligent Material Systems and Structures* **30**:6, 908-923. [Crossref]
8. Jagroop Singh, Somesh Kumar Sharma, Rajnish Srivastava. 2019. AHP-Entropy based priority assessment of factors to reduce aviation fuel consumption. *International Journal of System Assurance Engineering and Management* **10**:2, 212-227. [Crossref]
9. M Sivapragasam. 2019. Flow field behind a complex total pressure distortion screen. *Proceedings of the Institution of Mechanical Engineers, Part G: Journal of Aerospace Engineering* **60**, 095441001983786. [Crossref]
10. Yalin Pan, Jun Huang. 2019. Influences of airfoil profile on lateral-directional stability of aircraft with flying wing layout. *Aircraft Engineering and Aerospace Technology* **46**. . [Crossref]
11. Bharat Bhaga, Craig A. Steeves. 2019. Modeling hybrid polymer–nanometal lightweight structures. *Aerospace Systems* **29**. . [Crossref]
12. Hyoungjin Kim, May-Fun Liou. 2019. Flow simulation and drag decomposition study of N3-X hybrid wing-body configuration. *Aerospace Science and Technology* **85**, 24-39. [Crossref]
13. Puja Upadhyay, Khairul Q. Zaman. The Effect of Incoming Boundary Layer Characteristics On The Performance Of a Distributed Propulsion System . [Citation] [PDF] [PDF Plus]
14. Keisuke Sugaya, Taro Imamura. Grid Metrics Modification Approach for Flow Simulation around 3D Geometries on Cartesian CFD method . [Citation] [PDF] [PDF Plus]
15. Malcolm Dinovitzer, Calvin Miller, Adam Hacker, Gabriel Wong, Zach Annen, Padmassun Rajakareyar, Jordan Mulvihill, Mostafa El Sayed. Structural Development and Multiscale Design Optimization of Additively Manufactured UAV with Blended Wing Body Configuration Employing Lattice Materials . [Citation] [PDF] [PDF Plus]
16. Rubing Ma, Jianghao Wu. Multipoint and Multi-objective Optimization of Airfoil Considering Boundary Layer Ingestion 61-73. [Crossref]
17. Gang Yu, Dong Li, Yue Shu, Zeyu Zhang. The Engine Position Effect on SWB Airplane Aerodynamic Performance 201-210. [Crossref]
18. Alessio D'Ambros, Timoleon Kipouros, Pavlos Zachos, Mark Savill, Ernesto Benini. 2018. Computational Design Optimization for S-Ducts. *Designs* **2**:4, 36. [Crossref]
19. Zengyan Lian, Jianghao Wu. 2018. Aerodynamics and Propulsive Efficiency of a Blended-Wing-Body Aircraft with Distributed Propulsion System During Takeoff. *International Journal of Aeronautical and Space Sciences* **19**:4, 799-804. [Crossref]
20. Jagroop Singh, Somesh Kumar Sharma, Rajnish Srivastava. 2018. Managing Fuel Efficiency in the Aviation Sector: Challenges, Accomplishments and Opportunities. *FIIB Business Review* **7**:4, 244-251. [Crossref]
21. Lynnette M. Dray, Andreas W. Schäfer, Kinan Al Zayat. 2018. The Global Potential for CO 2 Emissions Reduction from Jet Engine Passenger Aircraft. *Transportation Research Record: Journal of the Transportation Research Board* **2672**:23, 40-51. [Crossref]

22. Alejandra Uranga, Mark Drela, David K. Hall, Edward M. Greitzer. 2018. Analysis of the Aerodynamic Benefit from Boundary Layer Ingestion for Transport Aircraft. *AIAA Journal* **56**:11, 4271-4281. [Abstract] [Full Text] [PDF] [PDF Plus]
23. Runze LI, Kaiwen DENG, Yufei ZHANG, Haixin CHEN. 2018. Pressure distribution guided supercritical wing optimization. *Chinese Journal of Aeronautics* **31**:9, 1842-1854. [Crossref]
24. E A Valencia, V H Alulema, V H Hidalgo. 2018. Weight assessment for a blended wing Body-Unmanned aerial vehicle implementing boundary layer ingestion. *IOP Conference Series: Materials Science and Engineering* **383**, 012068. [Crossref]
25. JiGuan G. Lin. Actuation Power Minimization Control . [Citation] [PDF] [PDF Plus]
26. Stephen T. McClain, Mario M. Vargas, Jen-Ching Tsao, Andy P. Broeren. Ice Roughness and Thickness Evolution on a Business Jet Airfoil . [Citation] [PDF] [PDF Plus]
27. Jason Qian, Juan J. Alonso. High-Fidelity Structural Design and Optimization of Blended-Wing-Body Transports . [Citation] [PDF] [PDF Plus]
28. Pavlos Kaparos, Savvas Koltsakidis, Pericles Panagiotou, Kyros Yakinthos. Experimental investigation of DBD plasma actuators on a BWB aerial vehicle model . [Citation] [PDF] [PDF Plus]
29. Julie Gauvrit-Ledogar, Sebastien Defoort, Arnault Tremolet, Franck Morel. Multidisciplinary Overall Aircraft Design Process Dedicated to Blended Wing Body Configurations . [Citation] [PDF] [PDF Plus]
30. Prajwal S. Prakasha, Pierluigi Della Vecchia, Pier Ciampa, Danilo Ciliberti, Dominique Charbonnier, Aidan Jungo, Marco Fioriti, Luca Boggero, Artur Mirzoyan, Kirill Anisimov, Mengmeng Zhang, Mark Voskuijl. Model Based Collaborative Design & Optimization of Blended Wing Body Aircraft Configuration : AGILE EU Project . [Citation] [PDF] [PDF Plus]
31. Feijia Yin, Arvind Gangoli Rao, Abhishek Bhat, Min Chen. 2018. Performance assessment of a multi-fuel hybrid engine for future aircraft. *Aerospace Science and Technology* **77**, 217-227. [Crossref]
32. Xiao-cui Wu, Yi-wei Wang, Chen-guang Huang, Zhi-qiang Hu, Rui-wen Yi. 2018. Numerical simulation of dynamic characteristics of a water surface vehicle with a blended-wing-body shape. *Journal of Hydrodynamics* **30**:3, 433-440. [Crossref]
33. Serhiy Bozhko, Christopher Ian Hill, Tao Yang. More-Electric Aircraft: Systems and Modeling 1-31. [Crossref]
34. Peifeng Li, Binqian Zhang, Yujin Tao, Zhenli Chen, Dong Li. 2018. Center Body Airfoil Design for Blended Wing Body Configuration. *Xibei Gongye Daxue Xuebao/Journal of Northwestern Polytechnical University* **36**:2, 203-210. [Crossref]
35. S.N. Skinner, H. Zare-Behtash. 2018. Study of a C-wing configuration for passive drag and load alleviation. *Journal of Fluids and Structures* **78**, 175-196. [Crossref]
36. Jerzy Żółtak. 2018. Multi-objective and multi-disciplinary design using evolutionary methods applied to aerospace design problems. *Proceedings of the Institution of Mechanical Engineers, Part G: Journal of Aerospace Engineering* **232**:4, 613-625. [Crossref]
37. Xiangyu Gu, Pier Davide Ciampa, Björn Nagel. 2018. An automated CFD analysis workflow in overall aircraft design applications. *CEAS Aeronautical Journal* **9**:1, 3-13. [Crossref]
38. Yann Denieul, Joël Bordeneuve, Daniel Alazard, Clément Toussaint, Gilles Taquin. 2018. Multicontrol Surface Optimization for Blended Wing–Body Under Handling Quality Constraints. *Journal of Aircraft* **55**:2, 638-651. [Abstract] [Full Text] [PDF] [PDF Plus]
39. Demetrios Kellari, Edward F. Crawley, Bruce G. Cameron. 2018. Architectural Decisions in Commercial Aircraft from the DC-3 to the 787. *Journal of Aircraft* **55**:2, 792-804. [Abstract] [Full Text] [PDF] [PDF Plus]
40. P. Panagiotou, S. Fotiadis-Karras, K. Yakinthos. 2018. Conceptual design of a Blended Wing Body MALE UAV. *Aerospace Science and Technology* **73**, 32-47. [Crossref]
41. Anirban Chaudhuri, John Jasa, Joaquim Martins, Karen E. Willcox. Multifidelity Optimization Under Uncertainty for a Tailless Aircraft . [Citation] [PDF] [PDF Plus]
42. Alexander W. Feldstein, David Lazzara, Norman Princen, Karen E. Willcox. Model Uncertainty: A Challenge in Nonlinear Coupled Multidisciplinary System Design . [Citation] [PDF] [PDF Plus]
43. Malcom Brown, Roelof Vos. Conceptual Design and Evaluation of Blended-Wing Body Aircraft . [Citation] [PDF] [PDF Plus]
44. Yu Cai, Imon Chakraborty, Dimitri N. Mavris. Integrated Assessment of Vehicle-level Performance of Novel Aircraft Concepts and Subsystem Architectures in Early Design . [Citation] [PDF] [PDF Plus]

45. Francesco Centracchio, Monica Rossetti, Umberto Iemma. 2018. Approach to the Weight Estimation in the Conceptual Design of Hybrid-Electric-Powered Unconventional Regional Aircraft. *Journal of Advanced Transportation* **2018**, 1. [Crossref]
46. Yanru He, Baowei Song, Yonghui Cao. 2018. Multi-Step Structural Optimization Design of Multi-Bubble Pressure Cabin in the Autonomous Underwater Vehicle with Blended-Wing-Body. *Xibei Gongye Daxue Xuebao/Journal of Northwestern Polytechnical University* **36**:4, 664. [Crossref]
47. Alessandro Sgueglia, Peter Schmollgruber, Emmanuel Benard, Nathalie Bartoli, Joseph Morlier. 2018. Preliminary Sizing of a Medium Range Blended Wing-Body using a Multidisciplinary Design Analysis Approach. *MATEC Web of Conferences* **233**, 00014. [Crossref]
48. Jacob Sliwinski, Alessandro Gardi, Matthew Marino, Roberto Sabatini. 2017. Hybrid-electric propulsion integration in unmanned aircraft. *Energy* **140**, 1407-1416. [Crossref]
49. M Z A Abd Latif, M A Ahmad, R E Mohd Nasir, W Wisnoe, M R Saad. 2017. An analysis on 45° sweep tail angle for blended wing body aircraft to the aerodynamics coefficients by wind tunnel experiment. *IOP Conference Series: Materials Science and Engineering* **270**, 012001. [Crossref]
50. Sami Ammar, Clément Legros, Jean-Yves Trépanier. 2017. Conceptual design, performance and stability analysis of a 200 passengers Blended Wing Body aircraft. *Aerospace Science and Technology* **71**, 325-336. [Crossref]
51. Hyoungjin Kim, Meng-Sing Liou. 2017. Flow simulation and optimal shape design of N3-X hybrid wing body configuration using a body force method. *Aerospace Science and Technology* **71**, 661-674. [Crossref]
52. Alejandra Uranga, Mark Drela, Edward M. Greitzer, David K. Hall, Neil A. Titchener, Michael K. Lieu, Nina M. Siu, Cécile Casses, Arthur C. Huang, Gregory M. Gatlin, Judith A. Hannon. 2017. Boundary Layer Ingestion Benefit of the D8 Transport Aircraft. *AIAA Journal* **55**:11, 3693-3708. [Abstract] [Full Text] [PDF] [PDF Plus]
53. Demetrios Kellari, Edward F. Crawley, Bruce G. Cameron. 2017. Influence of Technology Trends on Future Aircraft Architecture. *Journal of Aircraft* **54**:6, 2213-2227. [Abstract] [Full Text] [PDF] [PDF Plus]
54. Wenbiao Gan, Zhou Zhou, Xiaocui Zhang. 2017. Airframe/intake–exhaust integration design of flying wing using a multi-bump strategy. *Proceedings of the Institution of Mechanical Engineers, Part G: Journal of Aerospace Engineering* **231**:13, 2396-2407. [Crossref]
55. Jing Zhang, Xianfa Zeng, Lingyu Yang. 2017. Model-based analysis of boundary layer ingestion effect on lateral-directional aerodynamics using differentiated boundary conditions. *Proceedings of the Institution of Mechanical Engineers, Part G: Journal of Aerospace Engineering* **231**:13, 2452-2463. [Crossref]
56. Xiaobo Qu, Weiguo Zhang, Jingping Shi, Yongxi Lyu. 2017. A novel yaw control method for flying-wing aircraft in low speed regime. *Aerospace Science and Technology* **69**, 636-649. [Crossref]
57. David K. Hall, Arthur C. Huang, Alejandra Uranga, Edward M. Greitzer, Mark Drela, Sho Sato. 2017. Boundary Layer Ingestion Propulsion Benefit for Transport Aircraft. *Journal of Propulsion and Power* **33**:5, 1118-1129. [Abstract] [Full Text] [PDF] [PDF Plus]
58. David J. Arend, John D. Wolter, Stefanie M. Hirt, Andrew Provenza, John A. Gazzaniga, William T. Cousins, Larry W. Hardin, Om Sharma. Experimental Evaluation of an Embedded Boundary Layer Ingesting Propulsor for Highly Efficient Subsonic Cruise Aircraft . [Citation] [PDF] [PDF Plus]
59. Yan Wanfang, Jiang Kun, Zhang Jiang. Computational assessment of the effects of boundary layer ingestion in subsonic flow 507-511. [Crossref]
60. Y. Denieul, J. Bordeneuve-Guibé, D. Alazard, C. Toussaint, G. Taquin. 2017. Integrated design of flight control surfaces and laws for new aircraft configurations. *IFAC-PapersOnLine* **50**:1, 14180-14187. [Crossref]
61. Tyler Kraft, Travis Fields, Oleg A. Yakimenko. Feasibility of a Flying Wing-based Aerial Delivery Vehicle . [Citation] [PDF] [PDF Plus]
62. Timothy MacDonald, Matthew Clarke, Emilio M. Botero, Julius M. Vegh, Juan J. Alonso. SUAVE: An Open-Source Environment Enabling Multi-Fidelity Vehicle Optimization . [Citation] [PDF] [PDF Plus]
63. Brian M. Yutko, Neil Titchener, Christopher Courtin, Michael Lieu, Larry Wirsing, John Tylko, Chambers T. Jeffrey, Thomas W. Roberts, Clinton S. Church. Conceptual Design of a D8 Commercial Aircraft . [Citation] [PDF] [PDF Plus]
64. Francesco Faggiano, Roelof Vos, Max Baan, Reinier Van Dijk. Aerodynamic Design of a Flying V Aircraft . [Citation] [PDF] [PDF Plus]

65. May-Fun Liou, Hyoung Jin Kim, ByungJoon Lee, Meng-Sing Liou. Aerodynamic Design of Integrated Propulsion-Airframe Configuration of the Hybrid Wingbody Aircraft . [Citation] [PDF] [PDF Plus]
66. Pericles Panagiotou, Kyros Yakinthos. Parametric aerodynamic study of Blended-Wing-Body platforms at low subsonic speeds for UAV applications . [Citation] [PDF] [PDF Plus]
67. Oliverio Velazquez, Julien Weiss, François Morency. Preliminary investigation on stall characteristics of a Regional BWB for low speed approach . [Citation] [PDF] [PDF Plus]
68. Geoffrey Tanguy, David G. MacManus, Pavlos Zachos, Daniel Gil-Prieto, Eric Garnier. 2017. Passive Flow Control Study in an S-Duct Using Stereo Particle Image Velocimetry. *AIAA Journal* **55**:6, 1862-1877. [Abstract] [Full Text] [PDF] [PDF Plus]
69. Thomas A. Reist, David W. Zingg. 2017. High-Fidelity Aerodynamic Shape Optimization of a Lifting-Fuselage Concept for Regional Aircraft. *Journal of Aircraft* **54**:3, 1085-1097. [Abstract] [Full Text] [PDF] [PDF Plus]
70. Geoffrey Larkin, Graham Coates. 2017. A design analysis of vertical stabilisers for Blended Wing Body aircraft. *Aerospace Science and Technology* **64**, 237-252. [Crossref]
71. Vasileios S. Papapetrou, Ali Y. Tamijani, Daewon Kim. 2017. Preliminary Wing Study of General Aviation Aircraft with Stitched Composite Panels. *Journal of Aircraft* **54**:2, 704-715. [Abstract] [Full Text] [PDF] [PDF Plus]
72. Charles M. Boozer, Michael J. Van Tooren, Ali Elham. Multidisciplinary Aerodynamic Shape Optimization of a Composite Blended Wing Body Aircraft . [Citation] [PDF] [PDF Plus]
73. Ryan W. Plumley, Cale Zeune. Revolutionary Configurations: Technology Convergence Point . [Citation] [PDF] [PDF Plus]
74. Martijn Roelofs, Roelof Vos. Semi-Analytical Composite Oval Fuselage Weight Estimation . [Citation] [PDF] [PDF Plus]
75. Jason Qian. Automated Wingbox Structure Generation Through MATLAB . [Citation] [PDF] [PDF Plus]
76. Timothy MacDonald, Emilio Botero, Julius M. Vegh, Anil Variyar, Juan J. Alonso, Tarik H. Orra, Carlos R. Ilario da Silva. SUAVE: An Open-Source Environment Enabling Unconventional Vehicle Designs through Higher Fidelity . [Citation] [PDF] [PDF Plus]
77. Philipp Heinemann, Periklis Panagiotou, Patrick Vratny, Sascha Kaiser, Mirko Hornung, Kyros Yakinthos. Advanced Tube and Wing Aircraft for Year 2050 Timeframe . [Citation] [PDF] [PDF Plus]
78. R. J. H. Wanhill. Carbon Fibre Polymer Matrix Structural Composites 309-341. [Crossref]
79. A. Suleman, F. Afonso, J. Vale, É. Oliveira, F. Lau. 2017. Non-linear aeroelastic analysis in the time domain of high-aspect-ratio wings: Effect of chord and taper-ratio variation. *The Aeronautical Journal* **121**:1235, 21-53. [Crossref]
80. Yi Lu, Shu-Guang Zhang, Lian Hao, Hua-Yan Huangfu, Hang Sheng. 2016. System dynamics modeling of the safety evolution of blended-wing-body subscale demonstrator flight testing. *Safety Science* **89**, 219-230. [Crossref]
81. R E M Nasir, N S C Mazlan, Z M Ali, W Wisnoe, W Kuntjoro. 2016. A blended wing body airplane with a close-coupled, tilting tail. *IOP Conference Series: Materials Science and Engineering* **152**, 012021. [Crossref]
82. Rong Cui, Qiushi Li, Tianyu Pan, Jian Zhang. 2016. Streamwise-body-force-model for rapid simulation combining internal and external flow fields. *Chinese Journal of Aeronautics* **29**:5, 1205-1212. [Crossref]
83. Hugo Gagnon, David W. Zingg. 2016. Euler-Equation-Based Drag Minimization of Unconventional Aircraft Configurations. *Journal of Aircraft* **53**:5, 1361-1371. [Abstract] [Full Text] [PDF] [PDF Plus]
84. Lei Song, Hua Yang, Jingfeng Xie, Cong Ma, Jun Huang. 2016. Method for Improving the Natural Lateral-Directional Stability of Flying Wings. *Journal of Aerospace Engineering* **29**:5, 06016003. [Crossref]
85. Esteban Valencia, Victor Hidalgo, Jorge Cisneros. Design point analysis of a distributed propulsion system with boundary layer ingestion implemented in UAV's for agriculture in the Andean region . [Citation] [PDF] [PDF Plus]
86. Jaime Garcia-Benitez, Cristina Cuerno-Rejado, Rafael Gomez-Blanco. 2016. Conceptual design of a nonplanar wing airliner. *Aircraft Engineering and Aerospace Technology* **88**:4, 561-571. [Crossref]
87. Daniel C. Garmendia, Imon Chakraborty, Dimitri N. Mavris. 2016. Multidisciplinary Approach to Assessing Actuation Power of a Hybrid Wing–Body. *Journal of Aircraft* **53**:4, 900-913. [Abstract] [Full Text] [PDF] [PDF Plus]
88. Thomas A. Reist, David W. Zingg. Aerodynamic Design of Blended Wing-Body and Lifting-Fuselage Aircraft . [Citation] [PDF] [PDF Plus]
89. Garima Singh, Vassili Toropov, James Eves. Topology Optimization of a Blended-Wing-Body Aircraft Structure . [Citation] [PDF] [PDF Plus]

90. May-Fun Liou, David Gronstal, Hyoung Jin Kim, Meng-Sing Liou. Aerodynamic Design of the Hybrid Wing Body with Nacelle: N3-X Propulsion-Airframe Configuration . [Citation] [PDF] [PDF Plus]
91. Xiangyu Gu, Pier Davide Ciampa, Björn Nagel. High fidelity aerodynamic optimization in distributed overall aircraft design . [Citation] [PDF] [PDF Plus]
92. Geoffrey Tanguy, Pavlos Zachos, David G. MacManus, Daniel Gil-Prieto, Eric Garnier. Passive flow control study in a convoluted intake using Stereo Particle Image Velocimetry . [Citation] [PDF] [PDF Plus]
93. Martin Staggat, Antoine Moreau, Sebastien Guerin. Boundary Layer induced Rotor Noise using an Analytical Modal Approach . [Citation] [PDF] [PDF Plus]
94. Paul Peeters, James Higham, Diana Kutzner, Scott Cohen, Stefan Gössling. 2016. Are technology myths stalling aviation climate policy?. *Transportation Research Part D: Transport and Environment* **44**, 30-42. [Crossref]
95. Paul Okonkwo, Howard Smith. 2016. Review of evolving trends in blended wing body aircraft design. *Progress in Aerospace Sciences* **82**, 1-23. [Crossref]
96. Rudi Kirner, Lorenzo Raffaelli, Andrew Rolt, Panagiotis Laskaridis, Georgios Doulgeris, Riti Singh. 2016. An assessment of distributed propulsion: Part B – Advanced propulsion system architectures for blended wing body aircraft configurations. *Aerospace Science and Technology* **50**, 212-219. [Crossref]
97. Michael Kruger, R J. Huyssen, L Smith, J P. Meyer. Application of a low fineness ratio fuselage to an airliner configuration . [Citation] [PDF] [PDF Plus]
98. Gabriela J. Sanz-Douglass, Satchi Venkataraman. Parametric Study of Stiffener Variables on Post-Buckling Response of Frame-Stiffened Composite Panels . [Citation] [PDF] [PDF Plus]
99. Dawn C. Jegley, Marshall Rouse, Adam Przekop, Andrew E. Lovejoy. Testing of a Stitched Composite Large-Scale Pressure Box . [Citation] [PDF] [PDF Plus]
100. Patrick R. Shea, Jeffrey D. Flamm, Kurtis Long, Kevin D. James, Daniel Tompkins, Michael D. Beyar. Turbine Powered Simulator Calibration and Testing for Hybrid Wing Body Powered Airframe Integration (Invited) . [Citation] [PDF] [PDF Plus]
101. Anil Variyar, Thomas D. Economon, Juan J. Alonso. Multifidelity Conceptual Design and Optimization of Strut-Braced Wing Aircraft using Physics Based Methods . [Citation] [PDF] [PDF Plus]
102. Jing Zhang, Wenwen Kang, Ang Li, Lingyu Yang. 2016. Integrated flight/propulsion optimal control for DPC aircraft based on the GA-RPS algorithm. *Proceedings of the Institution of Mechanical Engineers, Part G: Journal of Aerospace Engineering* **230**:1, 157-171. [Crossref]
103. Aurélien Arntz, Olivier Atinault. 2015. Exergy-Based Performance Assessment of a Blended Wing–Body with Boundary-Layer Ingestion. *AIAA Journal* **53**:12, 3766-3776. [Abstract] [Full Text] [PDF] [PDF Plus]
104. Ralf Sturm, Martin Hepperle. 2015. Crashworthiness and ditching behaviour of blended-wing-body (BWB) aircraft design. *International Journal of Crashworthiness* **20**:6, 592-601. [Crossref]
105. Daniel C. Garmendia, Imon Chakraborty, Dimitri N. Mavris. 2015. Method for Evaluating Electrically Actuated Hybrid Wing–Body Control Surface Layouts. *Journal of Aircraft* **52**:6, 1780-1790. [Abstract] [Full Text] [PDF] [PDF Plus]
106. Chunya Sun, Baowei Song, Peng Wang. 2015. Parametric geometric model and shape optimization of an underwater glider with blended-wing-body. *International Journal of Naval Architecture and Ocean Engineering* **7**:6, 995-1006. [Crossref]
107. Rudi Kirner, Lorenzo Raffaelli, Andrew Rolt, Panagiotis Laskaridis, Georgios Doulgeris, Riti Singh. 2015. An assessment of distributed propulsion: Advanced propulsion system architectures for conventional aircraft configurations. *Aerospace Science and Technology* **46**, 42-50. [Crossref]
108. Crispijn Huijts, Mark Voskuijl. 2015. The impact of control allocation on trim drag of blended wing body aircraft. *Aerospace Science and Technology* **46**, 72-81. [Crossref]
109. T. I. Saeed, W. R. Graham. 2015. Design Study for a Laminar-Flying-Wing Aircraft. *Journal of Aircraft* **52**:5, 1373-1385. [Abstract] [Full Text] [PDF] [PDF Plus]
110. Chana Goldberg, Devaiah Nalianda, Riti Singh. Techno-economic and Environmental Risk Assessment of a Blended Wing Body with Distributed Propulsion . [Citation] [PDF] [PDF Plus]
111. Hyoungjin Kim, May-Fun Liou, Meng-Sing Liou. Mail-Slot Nacelle Shape Design for N3-X Hybrid Wing-Body Configuration . [Citation] [PDF] [PDF Plus]
112. Alexander Truong, Dimitri Papamoschou. Harmonic and Broadband Separation of Noise from a Small Ducted Fan . [Citation] [PDF] [PDF Plus]

113. Thomas A. Reist, David W. Zingg. Optimization of the Aerodynamic Performance of Regional and Wide-Body-Class Blended Wing-Body Aircraft . [Citation] [PDF] [PDF Plus]
114. David Rancourt, Sayan Ghosh, Dimitri N. Mavris, Simon Coggon. A Methodology to Create Approximate Models of Load Envelopes Under Uncertainty . [Citation] [PDF] [PDF Plus]
115. Nikhil Nigam, Sricharan K. Ayyalasomayajula, Xue Qi, Peter C. Chen, Juan J. Alonso. High-Fidelity Weight Estimation for Aircraft Conceptual Design Optimization . [Citation] [PDF] [PDF Plus]
116. Vivekanand Mukhopadhyay, Michael R. Sorokach. Composite Structure Modeling and Analysis of Advanced Aircraft Fuselage Concepts . [Citation] [PDF] [PDF Plus]
117. Vedant Singh, Somesh Kumar Sharma. 2015. Fuel consumption optimization in air transport: a review, classification, critique, simple meta-analysis, and future research implications. *European Transport Research Review* **7**:2. . [Crossref]
118. D. Verstraete. 2015. On the energy efficiency of hydrogen-fuelled transport aircraft. *International Journal of Hydrogen Energy* **40**:23, 7388-7394. [Crossref]
119. Payam Dehpanah, Amir Nejat. 2015. The aerodynamic design evaluation of a blended-wing-body configuration. *Aerospace Science and Technology* **43**, 96-110. [Crossref]
120. Yi Lu, Shu-Guang Zhang, Peng Tang, Lei Gong. 2015. STAMP-based safety control approach for flight testing of a low-cost unmanned subscale blended-wing-body demonstrator. *Safety Science* **74**, 102-113. [Crossref]
121. Esteban A Valencia, Devaiah Nalianda, Panagiotis Laskaridis, Riti Singh. 2015. Methodology to assess the performance of an aircraft concept with distributed propulsion and boundary layer ingestion using a parametric approach. *Proceedings of the Institution of Mechanical Engineers, Part G: Journal of Aerospace Engineering* **229**:4, 682-693. [Crossref]
122. Mushfiqul Alam, Martin Hromcik, Tomas Hanis. 2015. Active gust load alleviation system for flexible aircraft: Mixed feedforward/feedback approach. *Aerospace Science and Technology* **41**, 122-133. [Crossref]
123. John Hwang, Satadru Roy, Jason Kao, Joaquim Martins, William A. Crossley. Simultaneous aircraft allocation and mission optimization using a modular adjoint approach . [Citation] [PDF] [PDF Plus]
124. Daniel C. Garmendia, Dimitri N. Mavris. Power Efficient Trim Solutions for the Hybrid Wing Body in Approach Conditions . [Citation] [PDF] [PDF Plus]
125. Caroline Ingram, Hernando Jimenez, Jeff Schutte, Dimitri N. Mavris. Comparison of Advanced Vehicle Concepts through Pareto-Optimal Technology Sets . [Citation] [PDF] [PDF Plus]
126. Daniel C. Garmendia, Imon Chakraborty, Dimitri N. Mavris. Uncertainty Quantification for the Actuation Power Requirements of a Hybrid Wing Body Configuration with Electrically Actuated Flight Control Surfaces . [Citation] [PDF] [PDF Plus]
127. Afzal Suleman, Frederico Afonso, Jose Vale, Fernando Lau. Performance Based MDO of a Joined-Wing Regional Transport Aircraft (For Challenges in the Design of Joined Wings SPECIAL SESSION) . [Citation] [PDF] [PDF Plus]
128. Dawn C. Jegley, Alex Velicki. Development of the PRSEUS Multi-Bay Pressure Box for a Hybrid Wing Body Vehicle . [Citation] [PDF] [PDF Plus]
129. Andrew E. Lovejoy. Preliminary Weight Savings Estimate for a Commercial Transport Wing Using Rod-stiffened Stitched Composite Technology . [Citation] [PDF] [PDF Plus]
130. Masashi Kashitani, Yoshie Suganuma, Hisashi Date, Shinichiro Nakao, Yoshihiro Takita, Yutaka Yamaguchi. Experimental Study on Aerodynamic Characteristics of Blended-Wing-Body by a Wake Integration Method . [Citation] [PDF] [PDF Plus]
131. H. Baier, M. Hornung, B. Mohr, D. Paulus, Ö. Petersson, C. Rößler, F. Stroscher, T. Salmon. Conceptual Design 29-45. [Crossref]
132. Dawn C. Jegley, Alexander Velicki. Damage Arresting Composites 1-12. [Crossref]
133. Jorrit van Dommelen, Roelof Vos. 2014. Conceptual design and analysis of blended-wing-body aircraft. *Proceedings of the Institution of Mechanical Engineers, Part G: Journal of Aerospace Engineering* **228**:13, 2452-2474. [Crossref]
134. Fabio Furlan, Nicola Chiereghin, Timoleon Kipouros, Ernesto Benini, Mark Savill. 2014. Computational design of S-Duct intakes for distributed propulsion. *Aircraft Engineering and Aerospace Technology* **86**:6, 473-477. [Crossref]
135. Devaiah Nalianda, Riti Singh. 2014. Turbo-electric distributed propulsion – opportunities, benefits and challenges. *Aircraft Engineering and Aerospace Technology* **86**:6, 543-549. [Crossref]
136. Zhoujie Lyu, Joaquim R. R. A. Martins. 2014. Aerodynamic Design Optimization Studies of a Blended-Wing-Body Aircraft. *Journal of Aircraft* **51**:5, 1604-1617. [Abstract] [Full Text] [PDF] [PDF Plus]

137. A. N. Gissen, B. Vukasinovic, A. Glezer. 2014. Dynamics of flow control in an emulated boundary layer-ingesting offset diffuser. *Experiments in Fluids* **55**:8. . [Crossref]
138. Wan Fang Yan, Jiang Hao Wu, Yan Lai Zhang. 2014. Aerodynamic Performance of Blended Wing Body Aircraft with Distributed Propulsion. *Advanced Materials Research* **1016**, 354-358. [Crossref]
139. Chen Fang Cai, Jiang Hao Wu, Bin Liang. 2014. The Effect of Gust on Blended-Wing-Body Civil Aircraft. *Advanced Materials Research* **1016**, 359-364. [Crossref]
140. Sayan Ghosh, Hongjun Ran, Dimitri N. Mavris. A Generic Airfoil Design Method Based on a Naturally Bounded PARSEC Approach . [Citation] [PDF] [PDF Plus]
141. Vivekanand Mukhopadhyay. Hybrid-Wing-Body Vehicle Composite Fuselage Analysis and Case Study . [Citation] [PDF] [PDF Plus]
142. Daniel C. Garmendia, Imon Chakraborty, David R. Trawick, Dimitri N. Mavris. Assessment of Electrically Actuated Redundant Control Surface Layouts for a Hybrid Wing Body Concept . [Citation] [PDF] [PDF Plus]
143. Jason A. Corman, Dimitri N. Mavris. Characterization of an Aero-Structural Interaction for the Hybrid Wing Body Center Section in Conceptual Phase Structural Sizing . [Citation] [PDF] [PDF Plus]
144. A. N. Gissen, B. Vukasinovic, M. L. McMillan, A. Glezer. 2014. Distortion Management in a Boundary Layer Ingestion Inlet Diffuser Using Hybrid Flow Control. *Journal of Propulsion and Power* **30**:3, 834-844. [Abstract] [Full Text] [PDF] [PDF Plus]
145. Lynnette Dray, Antony Evans, Tom Reynolds, Andreas W. Schäfer, María Vera-Morales, Wolfram Bosbach. 2014. Airline fleet replacement funded by a carbon tax: An integrated assessment. *Transport Policy* . [Crossref]
146. Iftikhar B. Abbasov, V'iacheslav V. Orekhov. 2014. Computational modeling of multipurpose amphibious aircraft Be-200. *Advances in Engineering Software* **69**, 12-17. [Crossref]
147. Ramesh Agarwal, Zheming Zhang. 2014. Assessment and optimization of an airplane. *Aircraft Engineering and Aerospace Technology* **86**:2, 147-154. [Crossref]
148. Hugo Gagnon, David W. Zingg. High-fidelity Aerodynamic Shape Optimization of Unconventional Aircraft through Axial Deformation . [Citation] [PDF] [PDF Plus]
149. Thomas A. Reist, David W. Zingg. Aerodynamically Optimal Regional Aircraft Concepts: Conventional and Blended-Wing-Body Designs . [Citation] [PDF] [PDF Plus]
150. John R. Hooker. Design of a Hybrid Wing Body for Fuel Efficient Air Mobility Operations at Transonic Flight Conditions . [Citation] [PDF] [PDF Plus]
151. Gregory L. Roth, John Zhu, Robert D. Buchy. CREATETM-AV DaVinci Strategic Airlift Pilot Project . [Citation] [PDF] [PDF Plus]
152. Kristian Schmidt, Roelof Vos. A Semi-Analytical Weight Estimation Method for Oval Fuselages in Conventional and Novel Aircraft . [Citation] [PDF] [PDF Plus]
153. Kumar V. Singh, Laura A. McDonough, Raymond Kolonay, Jonathan E. Cooper. 2014. Receptance-Based Active Aeroelastic Control Using Multiple Control Surfaces. *Journal of Aircraft* **51**:1, 335-342. [Citation] [Full Text] [PDF] [PDF Plus]
154. Edwin Ordoukhanian, Azad M. Madni. 2014. Blended Wing Body Architecting and Design: Current Status and Future Prospects. *Procedia Computer Science* **28**, 619-625. [Crossref]
155. Tufail Habib. Multidisciplinary Product Decomposition and Analysis Based on Design Structure Matrix Modeling 409-423. [Crossref]
156. O. Scholz, M. Gariépy, J.Y. Trépanier. 2013. CFD optimization of an S-shaped engine diffuser with a boundary layer ingestion configuration. *Canadian Aeronautics and Space Journal* **59**:03, 93-105. [Crossref]
157. Hyoungjin Kim, Meng-Sing Liou. 2013. Shape design optimization of embedded engine inlets for N2B hybrid wing-body configuration. *Aerospace Science and Technology* **30**:1, 128-149. [Crossref]
158. Masahiro Kanazaki, Ryo Hanida, Takuya Nara, Makoto Shibata, Toshiyuki Nomura, Mitsuhiro Murayama, Kazuomi Yamamoto. 2013. Challenge of design exploration for small blended wing body using unstructured flow solver. *Computers & Fluids* **85**, 71-77. [Crossref]
159. Charles A. Mader, Joaquim R. R. A. Martins. 2013. Stability-Constrained Aerodynamic Shape Optimization of Flying Wings. *Journal of Aircraft* **50**:5, 1431-1449. [Abstract] [Full Text] [PDF] [PDF Plus]

160. Christopher Gedeon, Shane Huffer, Timothy T. Takahashi. Multi-Disciplinary Design of an Advanced Narrow-Body Transport Aircraft . [Citation] [PDF] [PDF Plus]
161. Rhea P. Liem, Charles A. Mader, Edmund Lee, Joaquim Martins. Aerostructural design optimization of a 100-passenger regional jet with surrogate-based mission analysis . [Citation] [PDF] [PDF Plus]
162. Stephen M. Waters, Mark Voskuijl, Leo L.M. Veldhuis, François J.J.M.M. Geuskens. 2013. Control allocation performance for blended wing body aircraft and its impact on control surface design. *Aerospace Science and Technology* **29**:1, 18-27. [Crossref]
163. Chen Fang Cai, Yong Ming Qin, Jiang Hao Wu. 2013. The Effect of Belly-Flap on Aerodynamic Performance of Blended Wing Body Civil Aircraft. *Applied Mechanics and Materials* **378**, 69-73. [Crossref]
164. Daniel Paulus, Christoph Wirth, Mirko Hornung. Blended Wing Body Aircraft - Recommendations from High Lift and Control Surface Design and Optimization . [Citation] [PDF] [PDF Plus]
165. Hugo Gagnon, David W. Zingg. Geometry Generation of Complex Unconventional Aircraft with Application to High-Fidelity Aerodynamic Shape Optimization . [Citation] [PDF] [PDF Plus]
166. Zhoujie Lyu, Joaquim Martins. RANS-based Aerodynamic Shape Optimization of a Blended-Wing-Body Aircraft . [Citation] [PDF] [PDF Plus]
167. Thomas A. Reist, David W. Zingg. Aerodynamic Shape Optimization of a Blended-Wing-Body Regional Transport for a Short Range Mission . [Citation] [PDF] [PDF Plus]
168. . From Tube and Wing to Flying Wing 121-155. [Crossref]
169. Ramesh Agarwal, Zheming Zhang. 2013. Assessment and optimization of an airplane's environmental impact. *Aircraft Engineering and Aerospace Technology* **85**:3, 199-206. [Crossref]
170. Yongliang Tian, Hu Liu, Haocheng Feng, Bo Wu, Guanghui Wu. 2013. Virtual Simulation-Based Evaluation of Ground Handling for Future Aircraft Concepts. *Journal of Aerospace Information Systems* **10**:5, 218-228. [Abstract] [Full Text] [PDF] [PDF Plus]
171. Vivekanand Mukhopadhyay. Hybrid Wing Body Pressurized Fuselage and Bulkhead Design and Optimization . [Citation] [PDF] [PDF Plus]
172. Roelof Vos, Maurice Hoogreef. Semi-Analytical Weight Estimation Method for Fuselages with Oval Cross-Section . [Citation] [PDF] [PDF Plus]
173. L. Leifsson, A. Ko, W.H. Mason, J.A. Schetz, B. Grossman, R.T. Haftka. 2013. Multidisciplinary design optimization of blended-wing-body transport aircraft with distributed propulsion. *Aerospace Science and Technology* **25**:1, 16-28. [Crossref]
174. Rodrigo Martinez-Val, Emilio Perez, Cristina Cuerno, Jose F Palacin. 2013. Cost-range trade-off of intermediate stop operations of long-range transport airplanes. *Proceedings of the Institution of Mechanical Engineers, Part G: Journal of Aerospace Engineering* **227**:2, 394-404. [Crossref]
175. Dimitri Papamoschou. Modeling of Jet-by-Jet Diffraction . [Citation] [PDF] [PDF Plus]
176. Trevor Laughlin, Jason Corman, Dimitri Mavris. A Parametric and Physics-Based Approach to Structural Weight Estimation of the Hybrid Wing Body Aircraft . [Citation] [PDF] [PDF Plus]
177. Zhoujie Lyu, Joaquim Martins. Aerodynamic Shape Optimization of a Blended-Wing-Body Aircraft . [Citation] [PDF] [PDF Plus]
178. Hamid Hefazi, Adam Vore, Daniel Dougherty. High lift flap design and testing for a tailless transport aircraft . [Citation] [PDF] [PDF Plus]
179. S. H. Cho, C. Bil, R. Adams. 2013. Design and optimisation of the external load bearing carry through structure of a columned multi bubble fuselage. *The Aeronautical Journal* **117**:1187, 97-108. [Crossref]
180. Yi LU, Shuguang ZHANG, Xueqing LI. 2012. A Hazard Analysis-based Approach to Improve the Landing Safety of a BWB Remotely Piloted Vehicle. *Chinese Journal of Aeronautics* **25**:6, 846-853. [Crossref]
181. Peng Cui, Jinglong Han. 2012. Prediction of flutter characteristics for a transport wing with wingtip devices. *Aerospace Science and Technology* **23**:1, 461-468. [Crossref]
182. B Mohr, D Paulus, H Baier, M Hornung. 2012. Design of a 450-passenger blended wing body aircraft for active control investigations. *Proceedings of the Institution of Mechanical Engineers, Part G: Journal of Aerospace Engineering* **226**:12, 1513-1522. [Crossref]
183. Zurriati Mohd Ali, Wahyu Kuntjoro, Wisnoe Wirachman. 2012. The Effect of Canard to the Aerodynamic Behavior of Blended Wing Body Aircraft. *Applied Mechanics and Materials* **225**, 38-42. [Crossref]

184. Stephen Andrews, Ruben Perez. Sizing of a Short Range Civil Transport Aircraft Considering Aero-Structural and Stability Effects . [Citation] [PDF] [PDF Plus]
185. Daniel Paulus, Simon Binder, Ögmundur Petersson, Horst Baier, Mirko Hornung. The Integration of an Efficient High Lift System in the Design Process of a Blended Wing Body Aircraft . [Citation] [PDF] [PDF Plus]
186. Zurriati Mohd Ali, Wahyu Kuntjoro, Wirachman Wisnoe. Effect of canard to the aerodynamic characteristics of Blended Wing Body airplane 696-700. [Crossref]
187. Peifeng LI, Binqian ZHANG, Yingchun CHEN, Changsheng YUAN, Yu LIN. 2012. Aerodynamic Design Methodology for Blended Wing Body Transport. *Chinese Journal of Aeronautics* **25**:4, 508-516. [Crossref]
188. David Arend, Gregory Tillman, Walter O'Brien. Generation after Next Propulsor Research: Robust Design for Embedded Engine Systems . [Citation] [PDF] [PDF Plus]
189. Z. Van Der Voet, F. J. J. M. M. Geuskens, T. J. Ahmed, B. Ninaber Van Eyben, A. Beukers. 2012. Configuration of the Multibubble Pressure Cabin in Blended Wing Body Aircraft. *Journal of Aircraft* **49**:4, 991-1007. [Citation] [PDF] [PDF Plus]
190. Michael Meheut, Aurelien Arntz, Gerald Carrier. Aerodynamic Shape Optimizations of a Blended Wing Body Configuration for Several Wing Planforms . [Citation] [PDF] [PDF Plus]
191. Kumar Singh, Laura McDonough, Raymond Kolonay, Jonathan Cooper. Receptance Based Active Aeroelastic Control Using Multiple Control Surfaces . [Citation] [PDF] [PDF Plus]
192. Charles Mader, Joaquim Martins. Optimal Flying Wings: A Numerical Optimization Study . [Citation] [PDF] [PDF Plus]
193. Roelof Vos, Jorrit van Dommelen. A Conceptual Design and Optimization Method for Blended-Wing-Body Aircraft . [Citation] [PDF] [PDF Plus]
194. M. E. Soulat. Parametric geometry representation to support aircraft design 1-17. [Crossref]
195. D. R. Hayhurst, K. T. Kedward, H. T. Soh, K. L. Turner. 2012. Innovation-led multi-disciplinary undergraduate design teaching. *Journal of Engineering Design* **23**:3, 159-184. [Crossref]
196. Tariq Saeed, William Graham. Conceptual Design for a Laminar-Flying-Wing Aircraft . [Citation] [PDF] [PDF Plus]
197. Hans Heerkens. 2012. Unmanned Cargo Aircraft: From Anywhere to Everywhere. *Engineering & Technology Reference* **1**:1. . [Crossref]
198. Mark Voskuijl, Jan de Klerk, Daan van Ginneken. Flight Mechanics Modeling of the PrandtlPlane for Conceptual and Preliminary Design 435-462. [Crossref]
199. Aldo Frediani, Vittorio Cipolla, Emanuele Rizzo. The PrandtlPlane Configuration: Overview on Possible Applications to Civil Aviation 179-210. [Crossref]
200. L. Cavagna, S. Ricci, L. Riccobene. 2011. Structural Sizing, Aeroelastic Analysis, and Optimization in Aircraft Conceptual Design. *Journal of Aircraft* **48**:6, 1840-1855. [Citation] [PDF] [PDF Plus]
201. Luca Cavagna, Sergio Ricci, Lorenzo Travaglini. 2011. NeoCASS: An integrated tool for structural sizing, aeroelastic analysis and MDO at conceptual design level. *Progress in Aerospace Sciences* **47**:8, 621-635. [Crossref]
202. M. Ali Zurriati, Kuntjoro Wahyu, Wirachman Wisnoe, E.M Nasir Rizal. 2011. The Effect of Canard on Aerodynamics of Blended Wing Body. *Applied Mechanics and Materials* **110-116**, 4156-4160. [Crossref]
203. Abraham Gissen, Bojan Vukasinovic, Michelle McMillan, Ari Glezer. Dynamics of Hybrid Flow Control in a Boundary-Layer-Ingesting Offset Diffuser . [Citation] [PDF] [PDF Plus]
204. Mark Drela. 2011. Design Drivers of Energy-Efficient Transport Aircraft. *SAE International Journal of Aerospace* **4**:2, 602-618. [Crossref]
205. Zurriati M. Ali, Wahyu Kuntjoro, Wirachman Wisnoe, Rizal Efendy M. Nasir, Firdaus Mohamad, Nor F. Reduan. The aerodynamics performance of Blended Wing Body Baseline-II E2 293-297. [Crossref]
206. Andrew Lovejoy, Marshall Rouse, Kim Linton, Victor Li. Pressure Testing of a Minimum Gauge PRSEUS Panel . [Citation] [PDF] [PDF Plus]
207. Yong Jie Zhang, Bin Tuan Wang. 2011. Non-Cylindrical Fuselage Structural Optimization of BWB Civil Aircraft. *Key Engineering Materials* **474-476**, 1736-1739. [Crossref]
208. Yong Jie Zhang, Peng Tao. 2011. Structural Analysis and Optimization of Aluminum Triple-Bubble Cabin. *Advanced Materials Research* **219-220**, 1117-1120. [Crossref]

209. Abraham Gissen, Bojan Vukasinovic, M. McMillan, Ari Glezer. Distortion Management in a BLI Inlet Diffuser using Synthetic-Jet Hybrid Flow Control . [Citation] [PDF] [PDF Plus]
210. Stephen Powell, András Sóbester, Phillip Joseph. Performance and Noise Trade-Offs on a Civil Airliner with Over-the-Wing Engines . [Citation] [PDF] [PDF Plus]
211. Nimeesha Kuntawala, Jason Hicken, David Zingg. Preliminary Aerodynamic Shape Optimization of a Blended-Wing-Body Aircraft Configuration . [Citation] [PDF] [PDF Plus]
212. Wirachman Wisnoe, M.A Zurriati, M Firdaus, R Nor Fazira, Rizal E.M. Nasir, Wahyu Kuntjoro. Experimental investigation of center elevator deflection on aerodynamics of UiTM's Baseline-I Blended Wing Body (BWB) unmanned aerial vehicle (UAV) 108-112. [Crossref]
213. Rizal E. M. Nasir, Wahyu Kuntjoro, Wirachman Wisnoe, Zurriati Mohd. Ali, Norfazira Reduan, Firdaus Mohamad, Ramzyzan Ramly. Static stability of Baseline-II blended wing- body aircraft at low subsonic speed: Investigation via computational fluid dynamics simulation 97-102. [Crossref]
214. R Martinez-Val, E Perez, J Puertas, J Roa. 2010. Optimization of planform and cruise conditions of a transport flying wing. *Proceedings of the Institution of Mechanical Engineers, Part G: Journal of Aerospace Engineering* **224**:12, 1243-1251. [Crossref]
215. Gaetan Kenway, Graeme Kennedy, Joaquim Martins. A CAD-Free Approach to High-Fidelity Aerostructural Optimization . [Citation] [PDF] [PDF Plus]
216. M. Hamdaoui, J. Chaskalovic, S. Doncieux, P. Sagaut. 2010. Using Multiobjective Evolutionary Algorithms and Data-Mining Methods to Optimize Ornithopters' Kinematics. *Journal of Aircraft* **47**:5, 1504-1516. [Citation] [PDF] [PDF Plus]
217. Rodrigo Martínez-Val, Cristina Cuerno, Emilio Pérez, Horacio H. Ghigliazza. 2010. Potential Effects of Blended Wing Bodies on the Air Transportation System. *Journal of Aircraft* **47**:5, 1599-1604. [Citation] [PDF] [PDF Plus]
218. G La Rocca, M J L van Tooren. 2010. Knowledge-based engineering to support aircraft multidisciplinary design and optimization. *Proceedings of the Institution of Mechanical Engineers, Part G: Journal of Aerospace Engineering* **224**:9, 1041-1055. [Crossref]
219. Gregory Herrick. Effects of Inlet Distortion on Aeromechanical Stability of a Forward-Swept High-Speed Fan . [Citation] [PDF] [PDF Plus]
220. C Cuerno-Rejado, L Alonso-Albir, P Gehse. 2010. Conceptual design of a medium-sized joined-wing aircraft. *Proceedings of the Institution of Mechanical Engineers, Part G: Journal of Aerospace Engineering* **224**:6, 681-696. [Crossref]
221. Leonard V. Lopes, Kenneth S. Brentner, Philip J. Morris. 2010. Framework for a Landing-Gear Model and Acoustic Prediction. *Journal of Aircraft* **47**:3, 763-774. [Citation] [PDF] [PDF Plus]
222. M. A. Sargeant, T. P. Hynes, W. R. Graham, J. I. Hileman, M. Drela, Z. S. Spakovszky. 2010. Stability of Hybrid-Wing-Body-Type Aircraft with Centerbody Leading-Edge Carving. *Journal of Aircraft* **47**:3, 970-974. [Citation] [PDF] [PDF Plus]
223. Naveed U. Rahman, James F. Whidborne. 2010. Propulsion and Flight Controls Integration for a Blended-Wing-Body Transport Aircraft. *Journal of Aircraft* **47**:3, 895-903. [Citation] [PDF] [PDF Plus]
224. John Lin, Gregory Jones, Brian Allan, Bryan Westra, Scott Collins, Cale Zeune. 2010. Wake Measurement Downstream of a Hybrid Wing Body Model with Blown Flaps. *International Journal of Flow Control* **2**:1, 1-20. [Crossref]
225. Jason E. Hicken, David W. Zingg. 2010. Aerodynamic Optimization Algorithm with Integrated Geometry Parameterization and Mesh Movement. *AIAA Journal* **48**:2, 400-413. [Citation] [PDF] [PDF Plus]
226. Gaetan Kenway, Ryan Henderson, Jason Hicken, Nimeesha Kuntawala, David Zingg, Joaquim Martins, Ross McKeand. Reducing Aviation's Environmental Impact Through Large Aircraft for Short Ranges . [Citation] [PDF] [PDF Plus]
227. R Martinez-Val, E Perez. 2009. Aeronautics and astronautics: Recent progress and future trends. *Proceedings of the Institution of Mechanical Engineers, Part C: Journal of Mechanical Engineering Science* **223**:12, 2767-2820. [Crossref]
228. Vikas Kumar, Farrukh S. Alvi. 2009. Toward Understanding and Optimizing Separation Control Using Microjets. *AIAA Journal* **47**:11, 2544-2557. [Citation] [PDF] [PDF Plus]
229. Gianfranco La Rocca, Michel J. L. Van Tooren. 2009. Knowledge-Based Engineering Approach to Support Aircraft Multidisciplinary Design and Optimization. *Journal of Aircraft* **46**:6, 1875-1885. [Citation] [PDF] [PDF Plus]
230. A. De Gaspari, S. Ricci, L. Riccobene, A. Scotti. 2009. Active Aeroelastic Control Over a Multisurface Wing: Modeling and Wind-Tunnel Testing. *AIAA Journal* **47**:9, 1995-2010. [Citation] [PDF] [PDF Plus]
231. Tariq Saeed, William Graham, Holger Babinsky, J Eastwood, Cesare Hall, Jerome Jarrett, M Lone, Keith Seffen. Conceptual Design for a Laminar Flying Wing Aircraft . [Citation] [PDF] [PDF Plus]

232. P.J. Masson, Taewoo Nam, T.P. Choi, P. Tixador, M. Waters, D. Hall, C.A. Luongo, D.N. Mavris. 2009. Superconducting Ducted Fan Design for Reduced Emissions Aeropropulsion. *IEEE Transactions on Applied Superconductivity* **19**:3, 1662-1668. [Crossref]

233. Luca Cavagna, Sergio Ricci, Luca Riccobene. A Fast Tool for Structural Sizing, Aeroelastic Analysis and Optimization in Aircraft Conceptual Design . [Citation] [PDF] [PDF Plus]

234. Aliya Valiyff, Maziar Arjomandi. An Investigation Into the Aerodynamic Efficiency of Tailles Aircraft . [Citation] [PDF] [PDF Plus]

235. Jason Hicken, David Zingg. Integrated Geometry Parameterization and Grid Movement Using B-Spline Meshes . [Citation] [PDF] [PDF Plus]

236. Jason Hicken, David Zingg. An Investigation of Induced Drag Minimization Using a Newton-Krylov Algorithm . [Citation] [PDF] [PDF Plus]

237. R. Alderliesten, R. Benedictus. 2008. Fiber/Metal Composite Technology for Future Primary Aircraft Structures. *Journal of Aircraft* **45**:4, 1182-1189. [Citation] [PDF] [PDF Plus]

238. Lars U. Hansen, Wolfgang Heinze, Peter Horst. 2008. Blended wing body structures in multidisciplinary pre-design. *Structural and Multidisciplinary Optimization* **36**:1, 93-106. [Crossref]

239. N U Rahman, J F Whidborne. 2008. A numerical investigation into the effect of engine bleed on performance of a single-spool turbojet engine. *Proceedings of the Institution of Mechanical Engineers, Part G: Journal of Aerospace Engineering* **222**:7, 939-949. [Crossref]

240. S. Saephan, C. P. Van Dam. 2008. Determination of Wing-Only Aircraft Tumbling Characteristics Through Computational Fluid Dynamics. *Journal of Aircraft* **45**:3, 1044-1053. [Citation] [PDF] [PDF Plus]

241. Sung Cho, Cees Bil, Javid Bayandor. Structural Design and Analysis of a BWB Military Cargo Transport Fuselage . [Citation] [PDF] [PDF Plus]

242. David A. Gebbie, Mark F. Reeder, Charles Tyler, Vladamir Fonov, Jim Crafton. 2007. Lift and Drag Characteristics of a Blended-Wing Body Aircraft. *Journal of Aircraft* **44**:5, 1409-1421. [Citation] [PDF] [PDF Plus]

243. Horacio H. Ghigliazza, Rodrigo Martinez-Val, Emilio Perez, Ladislav Smrcek. 2007. Wake of Transport Flying Wings. *Journal of Aircraft* **44**:2, 558-562. [Citation] [PDF] [PDF Plus]

244. G. E. Dorrington. 2007. Performance of non-rigid airships operating in the neutral buoyancy condition. *The Aeronautical Journal* **111**:1116, 89-103. [Crossref]

245. Daniel Crichton, Elena de la Rosa Blanca, Thomas Law, James Hileman. Design and Operation for Ultra Low Noise Take-Off . [Citation] [PDF] [PDF Plus]

246. Cesare A. Hall, Daniel Crichton. 2007. Engine Design Studies for a Silent Aircraft. *Journal of Turbomachinery* **129**:3, 479. [Crossref]

247. S Siouris, N Qin. 2007. Study of the effects of wing sweep on the aerodynamic performance of a blended wing body aircraft. *Proceedings of the Institution of Mechanical Engineers, Part G: Journal of Aerospace Engineering* **221**:1, 47-55. [Crossref]

248. R Martínez-Val, E Pérez, P Alfaro, J Pérez. 2007. Conceptual design of a medium size flying wing. *Proceedings of the Institution of Mechanical Engineers, Part G: Journal of Aerospace Engineering* **221**:1, 57-66. [Crossref]

249. Sergey Peigin, Boris Epstein. 2006. Computational Fluid Dynamics Driven Optimization of Blended Wing Body Aircraft. *AIAA Journal* **44**:11, 2736-2745. [Citation] [PDF] [PDF Plus]

250. A. Le Moigne, N. Qin. 2006. Aerofoil profile and sweep optimisation for a blended wing-body aircraft using a discrete adjoint method. *The Aeronautical Journal* **110**:1111, 589-604. [Crossref]

251. Syta Saephan, C.P. van Dam. Determination of Dynamic Stability Information Through Simulation of a Tumbling Tailless Aircraft . [Citation] [PDF] [PDF Plus]

252. A.P. Dowling, T. Hynes. 2006. Towards a silent aircraft. *The Aeronautical Journal* **110**:1110, 487-494. [Crossref]

253. Syta Saephan, C.P. van Dam. Simulation of the Tumbling Behavior of Tailless Aircraft . [Citation] [PDF] [PDF Plus]

254. Vikas Kumar, Farrukh S. Alvi. 2006. Use of High-Speed Microjets for Active Separation Control in Diffusers. *AIAA Journal* **44**:2, 273-281. [Citation] [PDF] [PDF Plus]

255. Leifur Leifsson, William Mason, Joseph Schetz, Raphael Haftka, Bernard Grossman. Multidisciplinary Design Optimization of Low-Airframe-Noise Transport Aircraft . [Citation] [PDF] [PDF Plus]

256. Adam Diedrich, James Hileman, David Tan, Karen Willcox, Zoltan Spakovszky. Multidisciplinary Design and Optimization of the Silent Aircraft . [Citation] [PDF] [PDF Plus]

257. James Hileman, Zoltan Spakovszky, Mark Drela, Matthew Sargeant. Aerodynamic and Aeroacoustic Three-Dimensional Design for a "Silent" Aircraft . [Citation] [PDF] [PDF Plus]

258. Robert Hall, Robert Biedron, Douglas Ball, David Bogue, James Chung, Bradford Green, Matthew Grismer, Gregory Brooks, Joseph Chambers. Computational Methods for Stability and Control (COMSAC): The Time Has Come . [Citation] [PDF] [PDF Plus]

259. David Gebbie, Mark Reeder, Charles Tyler, Vladimir Fonov, Jim Crafton. PSP-Based Experimental Investigation of a Blended Wing Body Aircraft . [Citation] [PDF] [PDF Plus]

260. Vivek Mukhopadhyay. Blended Wing Body (BWB) Fuselage Structural Design for Weight Reduction . [Citation] [PDF] [PDF Plus]

261. Charles Tyler, Mark Reeder, William Braisted, James Higgins, David Gebbie. Rapid Technology Focused Experimental and Computational Aerodynamic Investigation of a Strike Tanker . [Citation] [PDF] [PDF Plus]

262. N. Qin, A. Vavalle, A. Le Moigne, M. Laban, K. Hackett, P. Weinerfelt. 2004. Aerodynamic considerations of blended wing body aircraft. *Progress in Aerospace Sciences* **40**:6, 321-343. [Crossref]

263. David W. Zingg, Ömer L. Gülder. Technology Developments and Renewable Fuels for Sustainable Aviation 17-31. [Crossref]